Title

TEE HEMOGLOBIN CONTENT OF SINGLE ERYTHROCYTES IN CELL AGING AND HEMOPOIETIC DISTURBANCE

Author

Sondhaus, Charles Anderson.

Publication Date

1958-03-11

UCRL 8203

UNIVERSITY OF
CALIFORNIA

Radiation
Laboratory

THE HEMOGLOBIN CONTENT OF SINGLE ERYTHROCYTES IN CELL AGING AND HEMOPOIETIC DISTURBANCE

DISCLAIMER

UCRL-8203
Biology and Medicine

UNIVERSITY OF CALIFORNIA

Radiation Laboratory
Berkeley, California

Contract No. W-7405-eng-48

THE HEMOGLOBIN CONTENT OF SINGLE ERYTHROCYTES IN CELL AGING AND HEMOPOIETIC DISTURBANCE

Charles Anderson Sondhaus

(Thesis)

March 11, 1958

Printed for the U. S. Atomic Energy Commission

CONTENTS

THE HEMOGLOBIN CONTENT OF SINGLE ERYTHROCYTES IN CELL AGING AND HEMOPOIETIC DISTURBANCE

Charles Anderson Sondhaus

Donner Laboratory of Biophysics and Medical Physics
University of California, Berkeley, California

March 11, 1958

ABSTRACT

The method of microspectrophotography, which can measure the amount of light-absorbing substance in a single cell, was used to determine the hemoglobin concentration per unit area, the total dry mass of hemoglobin (Hb), and the cell diameter of single erythrocytes in dry smear preparations. Limitations in the technique are discussed from the point of view of the accuracy and applicability of the results obtained under the given conditions.

Erythrocyte populations were studied from four samples of normal human blood and from the blood of four individuals with polycythemia and chronic lymphatic leukemia. In another series of experiments, erythrocytes taken from four normal rabbits at several times before and after total-body irradiation with 600r of 230-kv(p) x-rays were studied as well; over 2000 red cells were measured in all. The relationships of Hb synthesis and red cell maturation, life span, and destruction in the normal and disturbed states as indicated in other studies suggested that effects on erythrocyte-size and Hb-content distribution patterns might be quantitatively observable by the microabsorption method.

In both the normal human and normal rabbit red cell populations, cellular Hb content paralleled cell diameter with a correlation coefficient of 0.5 to 0.8, while cellular Hb mass per unit area was inversely related to diameter with a lesser correlation of about 0.2 to 0.6. The correlations appeared to be altered in the abnormal states, the former decreasing and the latter increasing. The range of cell sizes was also changed. These trends were accompanied by indications of a generally lowered Hb content in all cell sizes, which was most marked in the smallest cells of the diseased populations relative to their normal counterparts. It is suggested that altered aging behavior may be reflected in decreased Hb retention of many individual cells in the populations of the diseased individuals.

At several times during the immediate post-irradiation period, changes in the above quantities were observed in the experimental animals. These are interpreted in terms of a temporary depression or cessation of new red cell formation and a constant aging of the existing population. A higher-than-normal initial Hb content, but a decreased retention of cellular Hb with time is suggested in the new cells which are present at 11 days after exposure, as early marrow

regeneration proceeds; but the young cells present in the population at 23 days post-irradiation may exhibit subnormal Hb content.

Normal reticulocytes were also studied, and were found on the average to be both larger (by 25%) and higher in total Hb mass (15 to 100%) than the average of the other older cells of a normal population, despite the lower concentration of Hb per unit area in the younger form and its high concentration in the oldest cells. It is inferred that there is a net loss of Hb in the normal process of aging in erythrocytes, accompanied by a size reduction, and in spite of the known occurrence of some additional Hb synthesis in the young circulating cells. The disturbances studied are thus interpreted in the light of such a correspondence between size and content distribution and age distribution in the red cell populations.

I. INTRODUCTION

a. Quantitative Cytophysical Studies in Hemopoiesis

In recent years, the study of single cells has been stimulated by the development of means of measurement sensitive enough to explore the relations of cellular composition, structure, and function on a quantitative basis. Since the amounts of material in an individual cell are on the ultramicroscale, the sensitivity of most microchemical methods is insufficient, and physical means, mainly using the properties of interaction of radiant energy and matter, have been most successful in meeting the requirements. The pioneer work is due to Caspersson (1936, 1950), who utilized the absorption of ultraviolet light as early as 1936, although Köhler had suggested its use in the microscope many years earlier (Köhler, 1904). Other recent approaches include that of microradiography with soft x-rays (Engström and Lindström 1947; Engström 1953), microradioautography of deposited radioisotopes in single cells (Doniach, Howard, and Pelc, 1953; Mazia, Plaut, and Ellis, 1955; Odeblad, 1952), and interference microscopy (Davies and Wilkins, 1952; Barer, 1952).

These methods usually consist of a modification in the use of the microscope, in which its classical function as an extension of the eye, and its use for qualitative, visual observation and classification of structure, has been augmented by a less inclusive but potentially more objective approach, the chemical identification and mass measurement of substances in situ. In using light itself as the quantitative tool, use must be made of one or more of the four properties of its wave motion: wavelength, amplitude, phase, and plane of vibration. Methods employing all four now exist, the most recent being that of interference microscopy (Dyson, 1959). The technique of microspectrophotometry makes use of the first two properties, by utilizing the high specific absorption of light at given wavelengths of certain classes of biological substances in the intact cell. Thus in the classical work of the Swedish school, Caspersson (1950), Hydén and Hartelius (1948), Noberger (1954), etc., have used the analyses of ultraviolet absorption curves of proteins and polynucleotides in a variety of material; Thorell (1947) studied the erythropoiesis and hemoglobin synthesis by using both the 260-mμ polynucleotide band and the characteristic near-ultraviolet or Soret-band absorption of hemoglobin at 415 mμ.

Parallel to these intrinsic absorption methods, the combination of microphotometry with staining by specific dyes has been developed, chiefly by Pollister and Ris (1947), Swift (1950), Alfert (1950), and others. In this approach a pigment, or more properly a chromophoric group, is added to the molecules of the biological material by any of several staining reactions which are selective towards one class of compounds only, and the resulting light absorption in the appropriate wavelength region is measured. Thus the Feulgen reaction is specific only to desoxyribose polynucleotides, the Millon reaction to the tryptophane and tyrosine groups in protein, and the dye azure B to nucleotides, permitting absorption measurements to be made which yield values proportional within limits to the content of these substances.

A number of applications of both UV and visual microphotometry have been made to studies of blood and hemopoiesis, for example, those of Thorell (1947, 1950), Jope (1949), Bussi et al. (1954), Ambs (1956), and Lagerlöf, Thorell, and Åkerman (1957). Thorell (1947) used photographic photometry in the far UV and a photoelectrical method in the Soret region to study normal and pathological hemopoiesis in mammals and man. His findings were: (1) the new formation of cellular protein during hemopoiesis takes place at an early stage of erythroblastic development in the presence of a high concentration ($>$ 5%) of ribose polynucleotides in the cytoplasm and nucleolar apparatus, in a manner resembling that of the other cells previously studied by the Caspersson group; (2) as maturation proceeds, this concentration of ribose polynucleotides decreases, while the declining growth activity of the individual blood cell appears to be caused by a reduced function of an unchanged amount of nucleolus-associated chromatin; (3) the specific differentiation process--the endocellular synthesis of hemoglobin (Hb)--does not start before the cytoplasmic ribose polynucleotide concentration has fallen from its initial value to below 0.5%. After this phase the main synthesis of Hb begins and the cellular content of Hb rises rapidly. On a quantitative basis, the stem cell development thus normally occurs in several different phases: (a) the phase of growth, (b) the phase of declining growth, (c) the differentiation phase, and (d) the phase of declining differentiation. These principles were further shown to be of a general character in the development of the unipotent stem cell into a functional tissue cell, and disturbances in the processes could be quantitatively demonstrated in certain pathological conditions of blood cell formation, specifically those of acute myeloid and lymphatic leukemia and in pernicious and hemorrhagic anemias.

In a later paper, Lagerlöf, Thorell, and Åkerman (1957) were able to demonstrate by the combined use of absorption measurements and micro-interferometry that the maximum rate of synthesis of the heme groups, as measured by the increase in total Soret band extinction per cell, followed in time that of the synthesis of protein, measured in terms of total cytoplasmic dry mass per unit area calculated from the phase-difference values. Both were determined over the time interval in cell growth during which the Hb mass per unit area increased from 10% to 90% of the total mass per unit area in the cytoplasm. This study again showed that the differentiation process of hemoglobinization was related to, but not synonymous with, the growth process itself.

In a study on the erythrocytes of peripheral blood, Ambs (1956) studied the total cellular hemoglobin content in populations of single red cells of normal adults, umbilical cord blood, and pernicious and hypochromic anemias. At the same time, measurements of cell diameters were obtained on the individual cells, as in the Price-Jones procedure (1933). Ambs described the relationship between diameter and Hb content as a loose one, cells of the same diameter varying in Hb content by as much as a factor of 2. On the average, however, the Hb content rose with increasing diameter, while he suggested that the average Hb content per unit area gave some indication of a decrease. In both cord blood and pernicious anemia, it was further concluded that, on the average, all the individual cells contained more Hb than did normal cells of the same diameter, and therefore the high Hb levels in these conditions were not due simply to those cells of largest diameter. He also found indications

that the population-distribution curves differed among the conditions studied, shapes suggestive of polymodality in cord blood and pernicious anemia indicating the possible existence of at least two morphologically distinct groups, but this possibility was not further explored. Ambs concluded that since exact data on volumes of cells in plasma was not available to settle the question of concentration, these curves were an appropriate means of gaining insight into the problem of subpopulations, since thickness changes in themselves had no effect on measurement of total Hb per cell.

b. Background of This Study

In the present study, an attempt has been made to apply the method of microspectrography to a further evaluation of the properties of Hb content and its relation to erythrocyte age and size in both normal populations and populations arising as a result of certain disturbances in erythropoiesis. Cell populations were studied in two types of disturbed conditions: (1) Disease, and (2) Recovery from radiation injury. In the first part of the study, cell populations of eight individuals were sampled, three of which represented different stages in the progression of polycythemia vera. In this condition, the erythroid elements and the other developmental series of blood-cell precursors are in a hyperplastic condition and produce red cells at high rates, leading to total masses of circulating erythrocytes which greatly exceed the normal amounts. Some evidence also exists that altered red cell life spans are involved in the condition. Another population was studied from a patient with chronic lymphatic leukemia, accompanied by anemia and showing evidence of a shortened red cell life span. These were compared with populations from four normal adult individuals, on one of whom samples were taken twice.

In the second series of experiments, six rabbits were used, five of which received a single sublethal whole-body dose of 230-kv(p) x-radiation; cell-population analyses were made on three of the irradiated animals at different times. After such an exposure the bone marrow first suffers a depression of proliferative activity and a degeneration of cells in the developmental series, and then becomes aplastic. This is followed by an active hemopoiesis, and regeneration of the marrow elements occurs in those animals which survive. Blood samples were taken from each animal before the exposure and at several intervals during the period in which these changes take place. Values could thus be compared with the control values in the same animal.

Erythrocytes arise as the end products of a series of divisions and differentiations of their precursor cells, mainly in the bone marrow but in some conditions in spleen and lymph nodes as well. The early erythroblast is the first of this group which is cytologically distinguishable from the precursor cells of the myeloid series; the monophyletic theory of Maximow, Gilmour, and others holds that both series stem from a common ancestor, the hemocytoblast or the lymphoidocyte (Gilmour, 1941), while the polyphyletic theory (Doan, Cunningham, and Sabin, 1925) places their origins in primitive reticuloendothelial cells which are stimulated to differentiate; the endothelial cells then produce the red cell series and the reticulum cells produce the white series. The early erythroblast divides and gives rise to the next cell type in

the series, the polychromatic erythroblast; Hb synthesis beings in these cells and each divides again to produce two orthochromatic erythroblasts. The latter cells proceed to synthesize Hb at a relatively rapid rate, after which they undergo nuclear pycnosis and loss. The cell size decreases uniformly throughout the series, while toward the end of this differentiation process, the rate of Hb synthesis begins to decrease.

At some point toward the end of the process, normally after the nuclei are lost, the cells leave the marrow sinusoid and appear in the circulating blood as reticulocytes. These young forms are distinguishable from the mature cells by the appearance of a dark reticular net when they are stained supra-vitally with brilliant cresyl blue. This form persists for several days, after which the characteristic biconcave disc shape is attained; the average lifetime of the mature form in the human is 120—130 days (Shemin and Rittenberg, 1946). The result of these processes is a peripheral blood cell population with an average normal content of Hb per cell of 28 to 32 x 10^{-12} g in humans.

There is evidence that the young enucleated red cells are still capable of some protein synthesis after entering the circulating blood (Nizet and Lambert, 1953; Austoni, 1954). By using the method of radioautography in which cells were incubated in solutions of Fe^{59} citrate, Austoni (1954) showed that mature erythrocytes incubated in the labelled citrate did not take up the isotope, but that all the erythroblastic maturation stages showed considerable uptake, and young marrow erythrocytes and reticulocytes took up smaller quantities. He concluded that if for some reason the erythrocyte were released while still immature, further Hb synthesis might take place in the circulating blood if the cells contained the precursor materials heme, protoporphyrin, globin, and iron.

In polycythemia vera, the bone marrow appears to be normal with respect to the relative numbers of cells in different maturation stages (Wasserman et al., 1952), but the total size of functional erythron is increased. In this respect, the marrow is not in a sense neoplastic, because its cells do not exhibit abnormalities as they do, for example, in the leukemias. By means of a life-span study with N^{15}-labelled glycine, London et al. (1949) found in one case of P. vera that the red cell lifetime was normal. On the other hand, using C^{14}-labelled glycine, Berlin, Lawrence, and Lee (1951) found evidence that the red cell life span remained normal in one case of chronic lymphatic leukemia but was reduced to 71 and 76 days in two cases of myelogenous leukemia, which therefore produced anemias since the production rate remained normal. In two cases of P. vera, they found that the graph of specific activity of Hb showed a rapid initial rise and fall in the first 15 days but was qualitatively similar to the normal from 40 to 200 days. By extrapolation and subtraction of the curve for the long-lived cells, the difference curve suggested that besides the presence of at least one class of cells with almost normal life span, a second class existed with a life span of only a few days. It was assumed in this analysis that the intracellular Hb was not exchangeable in either class of cells, and that removal of Hb and of erythrocytes from the circulation was the same process.

Huff et al. had also presented evidence in radioactive-iron studies that might indicate that the longevity of erythrocytes in P. vera is shortened (Huff et al., 1951). Berlin et al. thus concluded that distinct classes of both normal and short-lived cells existed in the population, and the rapid turnover of the short-lived cells must be largely responsible for the increased rate of iron turnover for Hb formation observed in P. vera.

These results suggested that the presence of more than one type of cell with respect to life span might lead to observably distinct classes of cells with altered size, Hb concentration, or Hb content. This might influence population distributions in terms of these quantities in a way which would not be apparent in the average values for the total population. Since an altered life span would parallel either an altered growth process, a different pattern of destruction, or both, it might also be supposed that the relationship of growth (shown by cell size) to differentiation (reflected in the extent of Hb synthesis) would be disturbed in a distinct class of abnormal cells, and that the disturbance might be quantitatively observable.

It has been known for some years that following a single dose of total-body radiation the processes of growth and differentiation in the erythroid series undergo marked inhibition within 24 hours. Hennessy and Huff (1950) showed that the uptake of Fe^{59} in erythrocytes of the rat was depressed by a factor of 10 in the first day, while Bloom and Bloom (1947) consider the red cell precursors to be the most radiosensitive of all the elements of mammalian bone marrow. In the rabbit, the depression reaches its greatest extent between the 10th and 15th day post-irradiation (Jacobsen et al., 1947), after which hemopoiesis is actively resumed. Between the 4th and 11th day after radiation, an "abortive rise" in numbers of reticulocytes, lymphocytes, and heterophils occurs in the rabbit; Jacobsen, Marks, and Lorenz (1949) suggest that it may represent a multiplication of cells that were injured at the time of radiation and then died after a limited number of divisions. These authors point out that this temporary increase in numbers of reticulocytes parallels the waves of regeneration in the marrow observed by Bloom and Bloom. In surviving animals, regeneration is not complete until several months have elapsed.

The erythrocyte values in peripheral blood of irradiated rabbits are less severely depressed than in other laboratory animals, and rabbits are relatively radioresistant. The LD500 value for the rabbit is 800r; at this dose, the reduction in number of circulating red cells by the 15th day is 27.5% (Jacobsen et al., 1947). During this time there is also a decrease in the plasma volume, which may mask the drop in total mass of erythrocytes (Prosser et al., 1947). It follows that the determination of red blood cell counts is a rather inaccurate measure of radiation effect during this period. The reduction of red cell mass results from (a) the lowered production of new cells, (b) the death of normally aging red cells, and (c) the loss of abnormal cells into lymphatic tissue and tissue spaces as well, since it has been found that labelled erythrocytes disappear more rapidly from the circulation of irradiated animals than from normal animals (Kahn and Furth, 1952). In this "aging" population of red cells, the changes in relative numbers of "older" and "newer" cells in the peripheral blood during the post-irradiation period might again be quantitatively observable as the appearance of subclasses of cells with altered Hb content or content-size relationships.

The aim of the present study was to determine whether such subclasses of older, newer, or abnormally behaving cells could be quantitatively differentiated from the normal cells with respect to morphology and Hb content, if the method of microspectrophotometry was applied to samples of the population of circulating red cells occurring in these dyscrasias and in the radiation-induced disturbances in erythropoiesis.

II. METHODS

a. Physical Principles

1. Absorption Laws

The spectral absorption of hemoglobin and other heme proteins occurs in two wave-length regions: that in the far ultraviolet is caused by the conjugated double bonds of the aromatic amino acids in the protein; and the other, in the near-ultraviolet and visible, is produced by the heme groups. The latter produce a system of bands, of which the most intense is the Soret band in the extreme violet, extending from about 390 mμ to 430 mμ. This absorption band is due to the porphyrin ring, and its exact position is determined by both the valence state of the central iron atom in the ring when combined with CO or O_2, and by changes in the double bonds of the side chains conjugated to the ring (Lemberg and Legge, 1949). There are slight differences in the bands between hemoglobins and myoglobins, but the Soret band of hemoglobin remains sensibly constant for many animal species. In solution, or when red cells are exposed to air, the Soret absorption-peak of hemoglobin is entirely due to the oxidized form, which is quite stable in the intact dried cell; this form thus resists denaturation in solution for 24 hours even at a pH of 9 (Jope, 1949).

If a layer of such an absorbing material is traversed by a parallel beam of monochromatic light, the light absorption which is produced varies with the number of absorbing molecules in the light path. Equal numbers of molecules reduce the intensity by equal fractions; hence the transmission through a number of layers of equal thickness and concentration of material will decrease logarithmically. This decrease in the intensity of the emerging beam is described by the Beer-Lambert law,

$$E = \log_{10} I_0/I = kcd, \qquad (1)$$

where the quantity E--called variously the extinction, density, or absorbance--is defined as the log of the ratio of incident intensity I_0 to the emergent intensity I. The extinction is linearly proportional to the concentration of substance per unit volume c, if Beer's law is obeyed, and to the thickness d as expressed by Lambert's law; where both laws hold, the extinction is proportional to their product. This in turn is linearly proportional to the total number of molecules of absorbing substance. The proportionality constant k is called the extinction coefficient; it is equal in value to the extinction of a solution of concentration 1 mg per cm^3 in a path length of 1 cm. The value of k is a function of the wave length, and the form of this function, the absorption curve, is characteristic of the substance.

The Beer-Lambert law does not hold for all degrees of concentration of many substances, owing to appearance of molecular interaction at high concentrations, but its range of validity may be determined for the material in question. For hemoglobin, Jope (1949) found that Beer's law was obeyed in the Soret region with concentrations extending from 0.019 per cent to 38.8 per cent; it is thus valid in erythrocytes where the concentration rarely exceeds the upper value.

2. Restrictions on the Determination of Absorbing Substance

Measurements of light absorption in microscopic images cannot be used to determine in any simple way the total amount of absorbing substance in a cell unless the extinction everywhere in the specimen is low, or unless the specimen extinction is uniform and its shape is simple (Davies, Wilkins, and Boddy, 1954). Errors are due to several main causes: (a) distortion of light intensities in the image relative to those in the object because of diffraction effects in inhomogeneous areas or in small objects; (b) reflections in the object or in the optical system which scatter some of the light out of the collecting lenses or redistribute it diffusely as glare; (c) some regions of the object being out of focus; (d) inhomogeneity in the over-all geometrical distribution of material in the object. The conditions under which valid measurements can be made have been the object of considerable study and some of these conditions will be summarized here.

The Beer-Lambert law applies strictly only to a slab of absorbing material of uniform thickness traversed by parallel rays of light, the size of the slab being large enough to treat the absorption by the laws of geometrical optics. In the microscope the formation of the image is described by geometrical optics down to an object size of roughly the order of the wave length of light. In this region, diffraction effects become increasingly important until, at an object size of about 0.1 λ, the light intensity is diffracted equally around the object and Rayleigh scattering occurs, directing a portion of the light energy outside even the highest-aperture objective lenses. This loss cannot easily be calculated, and it varies with the object size; the lower limit of size for which a valid absorption measurement can thus be obtained by geometrical optics has been shown by Caspersson (1936) to be about three times the wave length of the light used. This corresponds to the limiting size for which the distribution of light intensity in the image conforms within one or two per cent to that in the object, according to the Abbe theory of image-formation.

For larger objects, the distribution of intensity in the image is also influenced by: (1) the geometry of the object, (2) reflections and refractions in the object due to refractive-index changes at the boundaries of the object and the medium, and (3) the angle of convergence of the cone of light determined by objective and condenser aperture. In regard to these questions, Blout et al. (1950) give calculations which show that for small platelike areas the error between the case of a normally incident parallel beam and a convergent beam is small for low condenser apertures. Thorell (1947) showed that in convergent illumination, if the ratio of refractive indices of object and medium does not exceed 1.03, the intensity distribution in the image of a spherical, refractile, absorbing particle falls within 1% of that for a plane parallel plate of the same material with thickness equal to the sphere diameter and illuminated normally with parallel light, out of 0.85 of the sphere radius. For this value of index quotient, calculations from Fresnel's formulae by Caspersson and Engström (Thorell, 1947) show that the losses of light due to reflection in such refractile spheres will not exceed 0.7 per cent; i. e., an extinction of 0.003.

Another limitation arises from the fact that all but the thinnest objects will have some portion of the image out of focus to varying degrees. Davies and Walker (1953) showed that when an object is completely out of focus the per cent error in extinction is given approximately by 116 times the extinction. Thus for a small object or part of an object of average E about 0.1, if half the volume, say, is wholly out of focus, the error in that portion might reach 50 per cent, making the error in the total object about 25 per cent. If the mass of this small object is in turn part of the total mass of a larger object for which the remainder is entirely in focus, the total error will of course be reduced in the ratio of the smaller mass to the remainder.

3. Equations for Total Amount of Substance

The total amount of absorbing material in an object may be obtained with accuracy by integrating the optical density of extinction over all regions in the image, but this may be done only if the conditions discussed above are adequately met and the object lies within the depth of focus of the objective lens. Erythrocytes can be made to satisfy these conditions; their thickness rarely exceeds 3 micra and their optical extinction has a high degree of uniformity across the cell when viewed in the Soret region of hemoglobin absorption. Thus, special techniques, such as the crushing condenser (Davies, Wilkins, and Boddy, 1954) evolved to obviate some of the difficulties in thick inhomogeneous objects, are not required; in addition, the scanning and integration of extinction over the images are simplified by their regular circular shape.

The total mass m contained in a uniform slab of absorbing material of area a follows from Equation (1), because for $E = kcd$, then we have

$$m = cda = Ea/k . \tag{2}$$

Thus if both the extinction per unit area and the total area of the object can be measured, a value is obtained for the mass without regard to the thickness, which can seldom be accurately measured. The constant k is determined separately for the absorbing material. When the extinction varies across the object, a series of traces must be made across the image area and the total extinction must be summed:

$$m = \frac{w}{k} \frac{\sum_{i=1}^{n} \int_0^{\ell_i} E_x \, dx}{M_1 M_2 n} . \tag{3}$$

Here $\int dx$ is the length of the xth trace, E_x is the extinction, which varies along the trace, and w is the trace width on the projected image. (Figure 1a.) The integral $\int Edx$ is obtained by measuring the area under the x th trace, which can be accomplished in several ways. The magnifications M_1 and M_2 are those of the microscope and plate-scanning system, so that their product is the scale factor between a given distance in the specimen and on the trace.

The number of traces n can be chosen to suit the degree of heterogeneity in the object; in general the smaller the scanning aperture, both in length perpendicular to the trace (w) and in slit width, the higher the degree of accuracy in reducing distributional error in the measurement of total extinction of the resolved image.

Equation (3) can be modified in the case of objects with regular geometries and symmetrical distribution of material. For the absorption images of the circularly symmetric, biconcave disc-shaped erythrocytes a single scan across the diameter contains sufficient information to provide a close estimate of the total amount of hemoglobin in the cell. The expression for total mass is then (neglecting the magnification factors M_1 and M_2)

$$m = (\pi/k)E_{av}(\ell/2)^2 \quad . \tag{4}$$

This applies to cells of diameter ℓ whose extinction remains sufficiently constant over the total area to be treated as absorbing discs. In this case E_{av} is equal to A/ℓ, where $A = Ed\ell$, the area under the trace as before. Then one has

$$m = \pi A\ell/4k \quad . \tag{5}$$

For those cells in which the biconcavity is such as to produce a pronounced dip in the central part of the trace, the disc approximation cannot be used and the more general formula

$$m = 2\pi/k \int_0^{\ell/2} E_x x dx \tag{6}$$

must be employed, where the extinction E_x at distance x from the center of the trace of the cell image is read from the trace and the integral is evaluated numerically. (Figure 1b.)

In this study, photographic plates were scanned which had been individually calibrated in order to relate the plate darkening to the light intensity in each case. This relation, which is defined as the contrast or gamma of the emulsion, together with the magnification factors in the microscope and densitometer, and the plate-tracking and chart-paper-advance speeds, all introduce further numerical constants into the above expressions. These factors, together with their errors and those in the other quantities which were determined, are discussed in Part 3, where some typical determinations are presented.

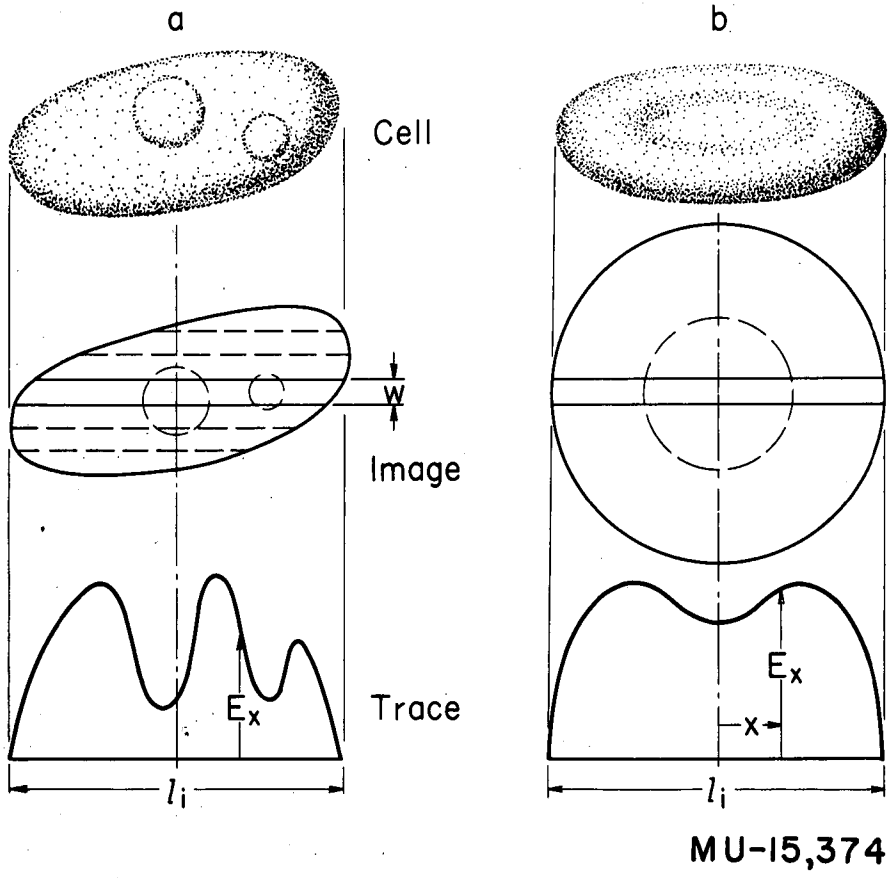

Fig. 1. Measurement of total extinction of
(a) irregular, and
(b) symmetrical objects.

b. Apparatus

1. Optical Equipment

The essential components for measurement of cellular light absorption are a suitable light source, a means of monochromatizing the light striking the specimen, a microscope optical system, and a recording device. In this investigation a tungsten ribbon-filament lamp was used as light source; it was focused by a collecting lens on the entrance slit of a Bausch and Lomb 250-mm-focal-length concave replica grating monochromator. This instrument is rated at f4.5, it has a linear dispersion of 66 Å /mm, and its spectral purity is described by the manufacturer as showing less than 0.1 per cent of stray light. A quartz fluorite condenser lens was fitted to the exit slit of the monochromator. Slit widths used were from 0.4 to 1.0 mm. A microscope stand was mounted to receive the emergent beam from the monochromator lens and the stand was fitted with an oil-immersion fluorite semi-apochromat objective lens of 40x magnification and N.A. 1.00, in combination with an achromatic condenser lens of N.A. 1.40, equipped with iris diaphragm. A compensating ocular of 15x magnification was used, with a tube length of 160 mm, while a first-surface-aluminized plane mirror was substituted for the usual mirror of the microscope.

The light source was imaged by the collective lens onto the entrance slit of the monochromator, while the exit lens of the monochromator imaged both the entrance and the exit slits onto the aperture stop at the back focal plane of the condenser lens in the microscope. The microscope condenser lens in turn formed an image of the monochromator exit-lens diaphragm in the specimen plane. In this use of the Köhler method of illumination, the microscope condenser diaphragm functions as the aperture stop of the system and the monochromator exit-lens diaphragm acts as the field stop, which is seen in the image plane. (Fig. 2.) The grating-area image also appears in the image plane, which is illuminated brightly and uniformly with monochromatic light.

By making the light path between immersion objective and condenser as free from index-of-refraction boundaries as possible, glare in this portion of the system was considerably reduced. At the same time the ratio of n_{cell} to n_{medium} was brought within a few per cent of unity, as can be demonstrated from the following consideration. The specific refractive increment of most proteins lies within the range 0.0018-0.0020 per g per 100 ml of solution (Adair, 1946) (that of hemoglobin is 0.00193). The average concentration of hemoglobin in the erythrocytes corresponds to about 97 per cent of the cell dry mass. If the dried cell preparation can be assumed to have shrunk in volume by even 20% or more and thus lost at least 1/3 of its water (,), it can be calculated that the index of refraction in the cell is roughly $n = (n_0 + ac) \geq 1.333 + 0.00193\ (45) \geq 1.42$. The index of refraction of the mineral immersion oil used being 1.565, it is seen that the ratio is $n_c/n_m \leq 1.09$, so that light losses due to reflection at the boundaries of cell and medium can be calculated by Fresnel's formula to be less than 2.0%. The practical absence of a Becke line in the images when racked through focus under dark-field illumination (Shillaber, 1944) confirmed this assumption.

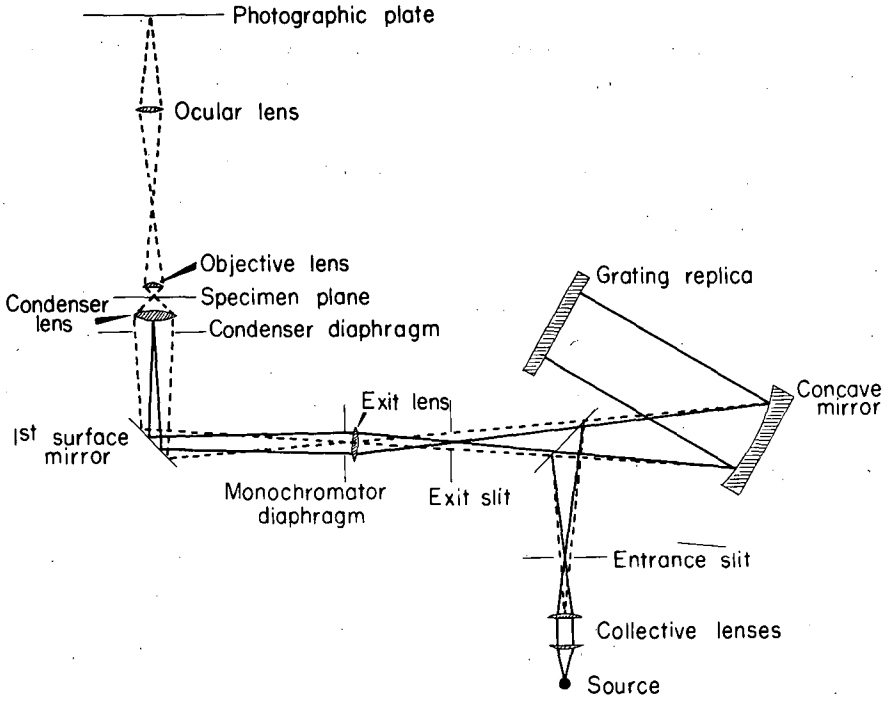

Fig. 2. Diagram of light path in the optical system

2. Plate Recording and Calibration

A photomicrographic camera and stand completed the microspectrophotometric system. A Bausch and Lomb photomicrographic equipment model L was used which had been modified to allow individual calibration of each photographic plate in the following way. A minature electric motor was mounted on an adjustable brass arm so that the motor axis could be aligned perpendicular to the plane of the photographic plate. A rotating-sector disc was next constructed of 1/16-in. brass and mounted on the motor shaft so that its plane of rotation was approximately 9 mm above that of the plate surface, thus allowing the cassette with plate to be inserted and removed. (Fig. 3.)

The sector was constructed to provide 14 levels of light intensity, the center area being opaque and the successive steps toward the periphery being in equal decrements of extinction, i.e., logarithmically related in terms of per cent transmission. For each exposure the rotation of the sector thus provided a calibration curve which related plate darkening to extinction of the beam. To minimize possible stroboscopic effects due to synchronization with line-current alternation, the sector motor was energized separately by a dry-cell battery. The sector was rotated at a speed fast enough to eliminate intermittency effects on plate darkening; the critical power limit is given by Walker (1956) as 40 interruptions per exposure, which was easily met with the exposure times used.

Kodak Process emulsion was used in most of the determinations, and the plate size used was 2-1/4 x 3-1/4 in. Other emulsions were tested, including Kodak spectroscopic 103 - a0, and Kodak Spectrum Analysis Nos. 1 and 2. Both Process and SA-2 were found to be quite satisfactory, in regard to speed, gamma, graininess, and spectral response in the ultra-violet. A study was made of development time versus film response in which development was varied from 4 to 16 minutes, using several developers including Kodak D-19, D-11, and D-76. It was found that 4 minutes' development in D-76 at 68°F gave the best combination of contrast and latitude in the calibration curves. For the light source and optics used, exposure times of 90 to 180 sec were necessary. After development, the plates were rinsed for 30 seconds in a shortstop bath of 2% glacial acetic acid, fixed 20 min in Kodak acid fixer, and washed one hour in running water. A rinse in photoflow solution was then followed by drying in air at room temperature.

3. Photometric Scanning of Plates and Integration of Trace Areas

The plates were scanned with an automatic recording microphotometer (Applied Research Labs--Dietert) which had been modified to receive the plates at the scanning head by the addition of a square of optically flat glass on the plate-holder stage. The distance between clamps on the stage was extended by adding arms of 1/8-in. brass to the existing framework; the plate to be scanned could then be mounted in any angular position on the plane of the glass.

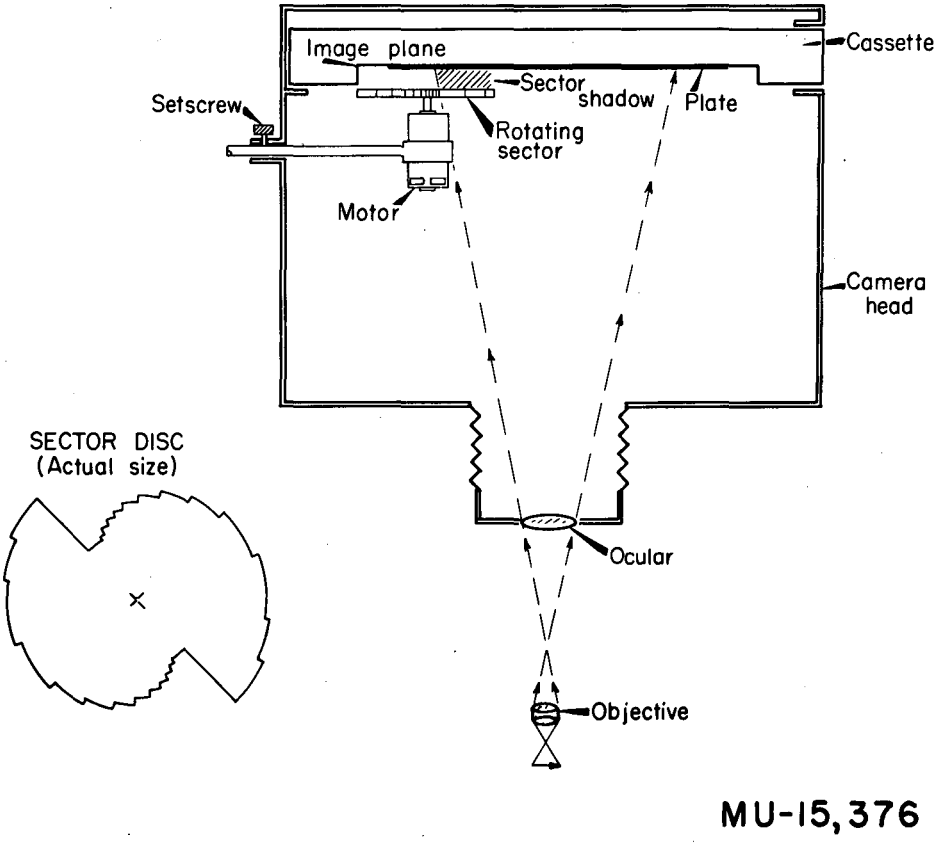

Fig. 3. Plate-calibration system.

The distance from the emulsion surface on the plate to the slit on the photometer head was approximately 0.2mm. The scanning slit width used was 20μ, and its length was 0.7mm, which resulted in an area of $0.025\mu^2$ being scanned on the scale of the cell at the magnification used. The images were scanned at a speed of 3.6mm per minute. The output of the photomultiplier tube which received the transmitted beam in the photometer head was applied to a bridge circuit which, in turn, caused a linear amplifier to drive a Leeds and Northrup strip chart recorder, having a paper speed of 2.5 in./min. The system plotted light intensity through the plate in terms of per cent transmission. Zero and 100-per-cent values set on the bridge circuit were found to remain constant of 0.5% during a 20-minute operating period once the components of the recording system had reached thermal equilibrium. The resulting ratio of scanning distance was 1 inch on paper to 1.45mm on the plate.

The light intensity in a photometer trace across a cell image was plotted in terms of specular per cent transmission. On each plate a trace of the sector steps provided a calibration curve relating the light transmission of the darkened emulsion to the sector-extinction values along the path of the trace. By a careful control of exposure and development conditions, the images of the cells could be made to fall almost entirely on the linear portion of the calibration curve, so that at any point in an image, the difference in per cent transmission between that point and the background was linearly proportional to the light-extinction value in the cell at that point. Only those plates in which this linear relationship was followed to within 90% of the maximum light-transmission value in the images were selected for scanning. For those portions of the traces where the per cent transmission exceeded the region of linearity, a correction factor was applied. As the linear relationship then held, the area under the curve was proportional to the total extinction along the path of the trace. Determination of the areas in each case could be accomplished in several ways: for example, by planimetry, by cutting and weighing of the trace areas on the paper, or by the use of an electronic analog integrating device. This last device applies a voltage proportional to the output voltage of the photometer tube to the condenser of an electrometer circuit; this method was chosen as best suited to the system. Accordingly, an integrating electrometer with slide-wire potentiometer was mechanically coupled to the servomotor shaft of the first recorder, and the accumulation of charge with time then provided the analog of the total area under the trace as the image was scanned. This quantity was recorded simultaneously with the trace itself. In this way, for each cell image traced, 2 quantities were determined; the trace length and the total extinction under the trace. These data formed the basis of the analyses.

c. Technique and Accuracy

Figure 4 is a positive of a plate photographed at 415 mμ, showing a typical field of cell-absorption images and the image of the rotating sector. The line indicates the path of scanning along the sector steps, while the short lines illustrate the locations of traces across the cell images. On most plates only about the central half of the total illuminated area was used. It was found that the background density in this region could be kept constant within 2% transmission by careful and repeated alignment of the optical system and centering of the monochromator and objective lenses, and by accurate focussing of specimen and image of monochromator diaphragm in the image plane. The focussing was accomplished for the plane of the

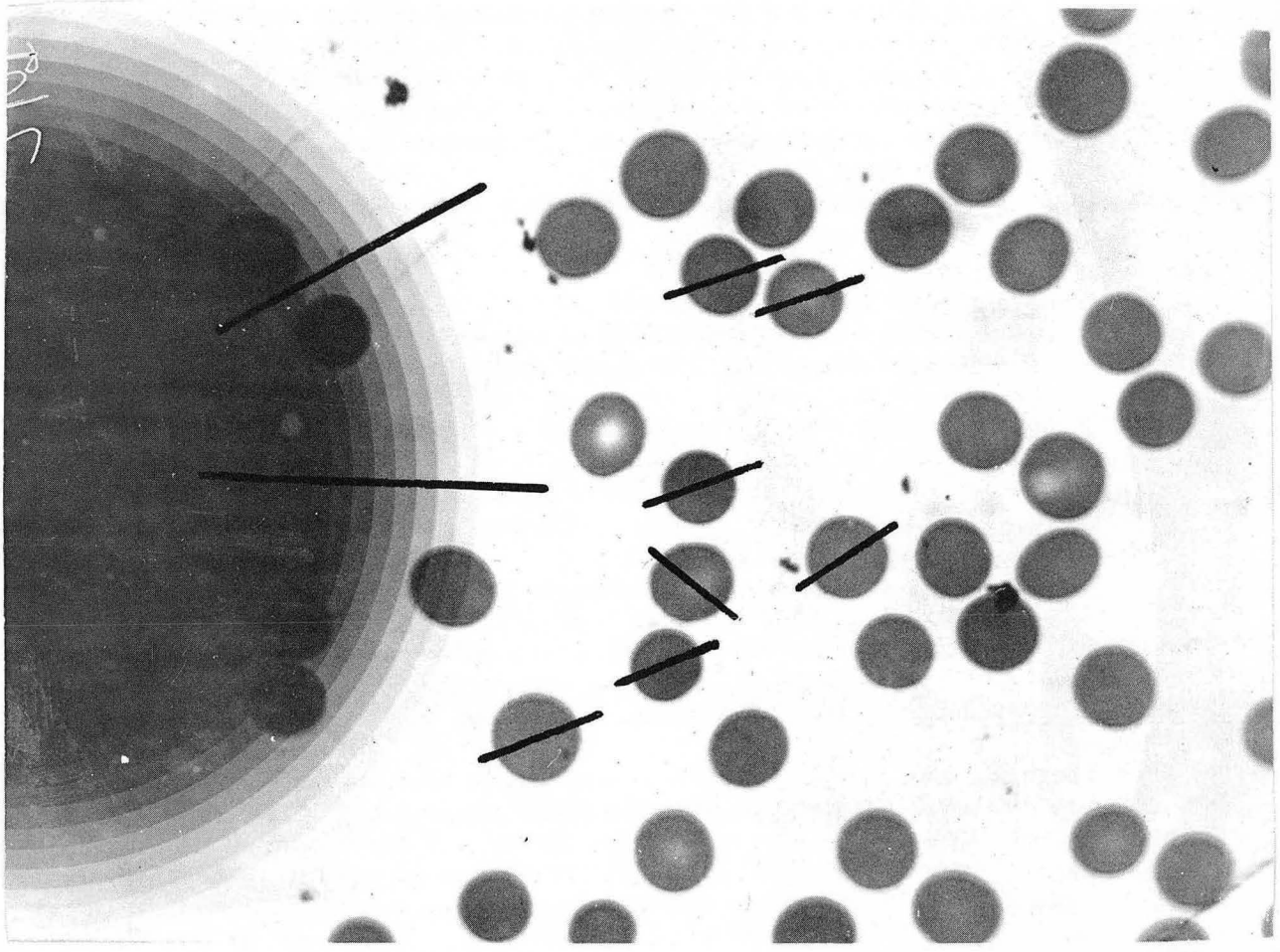

ZN-1943

Fig. 4. Absorption images of erythrocytes photographed at 415 mμ (positive of original plate taken at 745 X).

photographic plate by the use of a hand telescope by which the images were focussed sharply on the ground glass screen of the camera box. Glass strips cemented to the screen with Canada balsam provided a clear area for direct viewing of fine detail.

Figure 5a illustrates the traces resulting from a scan of the sector steps and two cell images, while Fig. 5b shows the resulting calibration curve for that plate. It is seen that the plate latitude is such as to produce linearity of response over the region 30—75 per cent transmission, which corresponds to an extinction above background of approximately 0.4 unit. This was found to hold for nearly all the plates used. [The slope of the calibration curve could be repeatedly measured with a standard error of 2%.]

On one image the peaks of highest extinction extend beyond the linear range. The method of correction for non-linearity is illustrated on the calibration curve in Fig. 5b. For each point in the image-transmission curve which fell on the curved portion of the calibration plot, the transmission reading on the ordinate was corrected by a small amount to correspond to the given extinction on the abscissa as shown. This resulted in a small increment of area B, which made the entire area in Fig. 5a linearly proportional to the quantity $\int E d\ell$. The uncorrected area A was obtained by means of the integrating electrometer, which plotted the integral curve as the area under the image trace was swept out. This curve is also shown for each cell image in Fig. 5a. (The integral chart scale differs from that of the images.) In those images where corrections were applied, the areas B were then measured by planimetry. Plates where the areas B would be on the average greater than 10% of A were discarded.

The integrating electrometer was calibrated by plotting its reading for a given area on the chart against the value obtained by planimetry of the same area. Since the input to the electrometer was determined by the position of the slide wire on the image-trace recorder and the coupling was mechanical, the integrator would measure any arbitrary area which adjustment of the recorder bridge circuit caused it to sweep out. Areas from 1 to 30 square inches were thus measured on the electrometer. A series of 24 such measurements was made; the resulting calibration curve is shown in Fig. 6. The values of the ratio ranged from 0.228 to 0.236, and the mean value used was 0.232 ± 0.004 in.^{2} per scale div on the integrator chart.

In order to measure linear dimensions on the cell images, photographs were made using an ocular micrometer under the same conditions as those at which the specimen photographs were made, and the image of the micrometer scale was scanned with the microphotometer. Distances were measured between the points of half peak height for a series of peaks separated by ten micrometer-scale divisions in each determination. The ocular micrometer, in turn, was calibrated against a stage micrometer under the same conditions. With the magnifications, microphotometer scanning, and chart speeds used, it was found that one inch on the recorded trace was equal to 1.45 ± 0.05 mm on the plate, or to 1.95 ± 0.08 microns in the specimen plane. The magnification factor in the photomicrographic system was thus 745 ± 30, and the total magnification of the traces was about 13000. The cell diameters were also measured at half peak height as shown. These factors

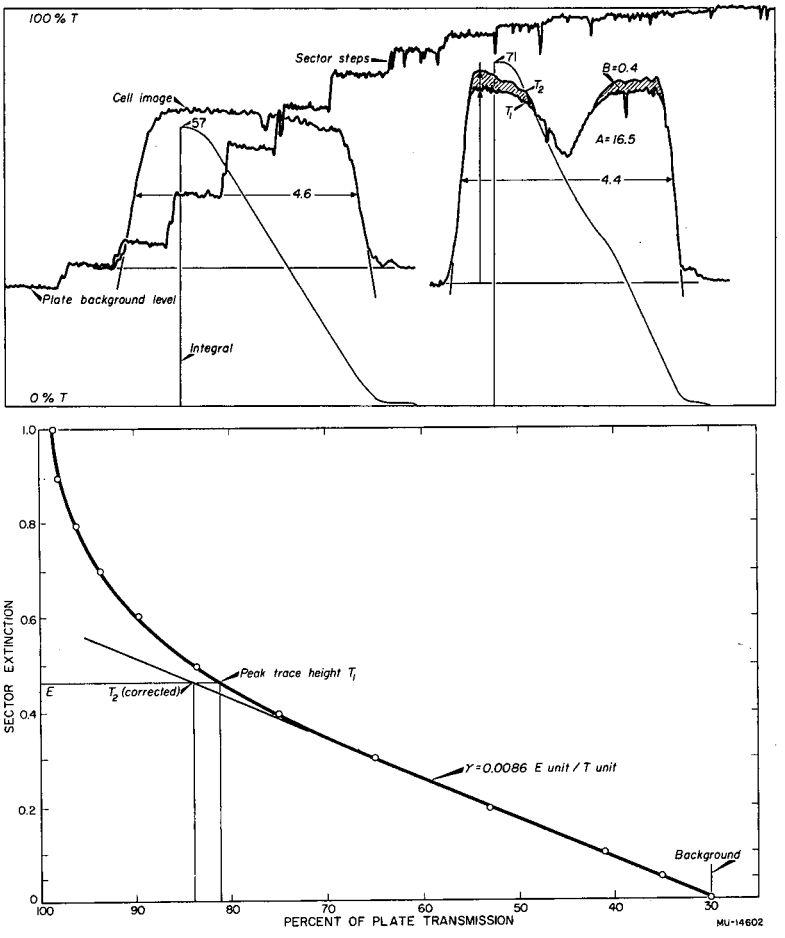

Fig. 5a. Photometer traces of sector step image and two red cell images, and integral traces of the area under the image curves. (The scale and position of the latter are arbitrary.)

5b. Plate-calibration curve resulting from the plot of sector-step extinctions vs percent transmission on plate.

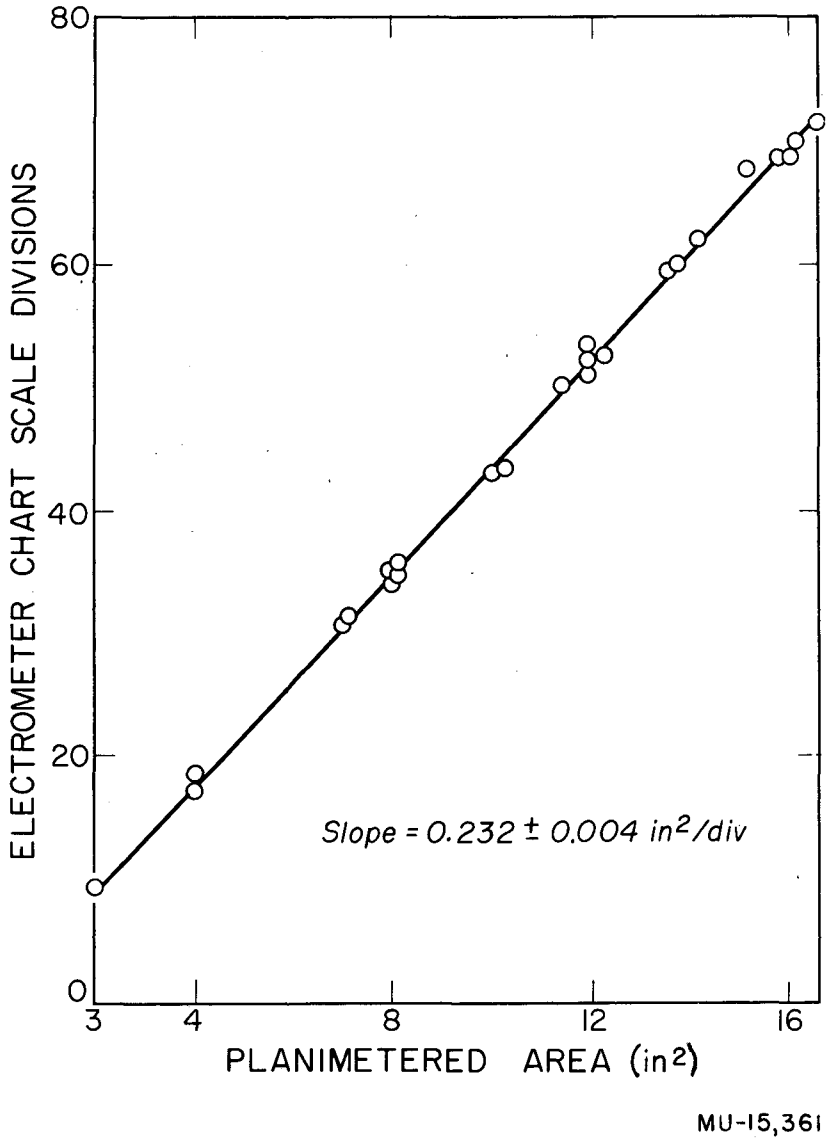

Fig. 6. Calibration curve for integrating electrometer.

were checked several times during the course of the measurements, and were found to remain within the indicated ranges.

The monochromator and microscope were tested for stray light (glare) and for degree of spectral purity in two ways (Swift and Rasch, 1956). By use of doublet emission lines of a mercury arc at 577 and 579 mμ, the intensity at the eyepiece was measured at wave lengths on either side and across the region of the emission lines, by using slit widths from 0.1 to 1.0mm. Figure 7 shows two graphs of intensity versus wave length for 0.2 and 0.4mm slit width. Intensities were measured by mounting a 1P21 photomultiplier tube in a lighttight head on the eyepiece of the microscope and noting the readings on the microammeter of a dc amplifier receiving the output of the cell. It was found, for example, that the band width at half-maximum intensity was 2.1 mμ for monochromater slit width of 0.4mm, and reached 6.5 mμ for a slit width of 1.0mm. The intensity at wave lengths greater than twice these band widths on either side of the line was 0.5% of the maximum values, indicating that glare on the monochromator was low enough to be insignificant.

To test for glare due to internal reflection and scattered light in the microscope system, small opaque objects such as dust particles and finely crushed graphite were mounted in immersion oil on a slide, a cover slip was placed on the preparation, and their images were photographed in the same manner as were the specimens. Transmissions in the central areas of such images were always above 95%, indicating that the intensity of scattered reflected light was again about 0.5% of that in the adjacent background.

Determinations of absorption coefficient for hemoglobin, evaluation of inhomogeneity and nonspecific absorption in the cell images, and discussions of hemoglobin absorption curves in the single cells are presented in Part III.

Summarizing the foregoing discussion, in which errors in some of the calibrations have been described, one may estimate a total random error in the method as follows. Equation (5) is the basis for total mass determination in any cell. The measurement of ℓ on the chart and k are subject to standard errors of 2% each as before stated. In addition, the measurement of total area consists of several steps; measurement of trace height on integrator chart i, multiplication of this by the conversion factor ϵ, and planimetering the smaller area B resulting from correction by use of the calibration curve. To convert to extinction units, the total area must be multiplied by the scale factor converting trace height to transmission units on the chart, and by the plate-calibration factor which, in turn, transforms transmission to extinction. The final equation for total mass may be summarized as follows:

$$m = \pi \alpha \gamma \beta^2 (\epsilon i + B) \ell / 4k,$$

where

$\alpha = 12.1 \pm 0.1$ T units/in.,

$\gamma = 0.0090 \pm 0.002$ E unit/T unit (varied with plate),

$\beta = 1.95 \pm 0.08$ μ/in.,

$\epsilon = 0.232 \pm 0.004$ in.^{2}/div,

$k = 6.5 \pm 0.1$ $\mu^2/\mu g$,

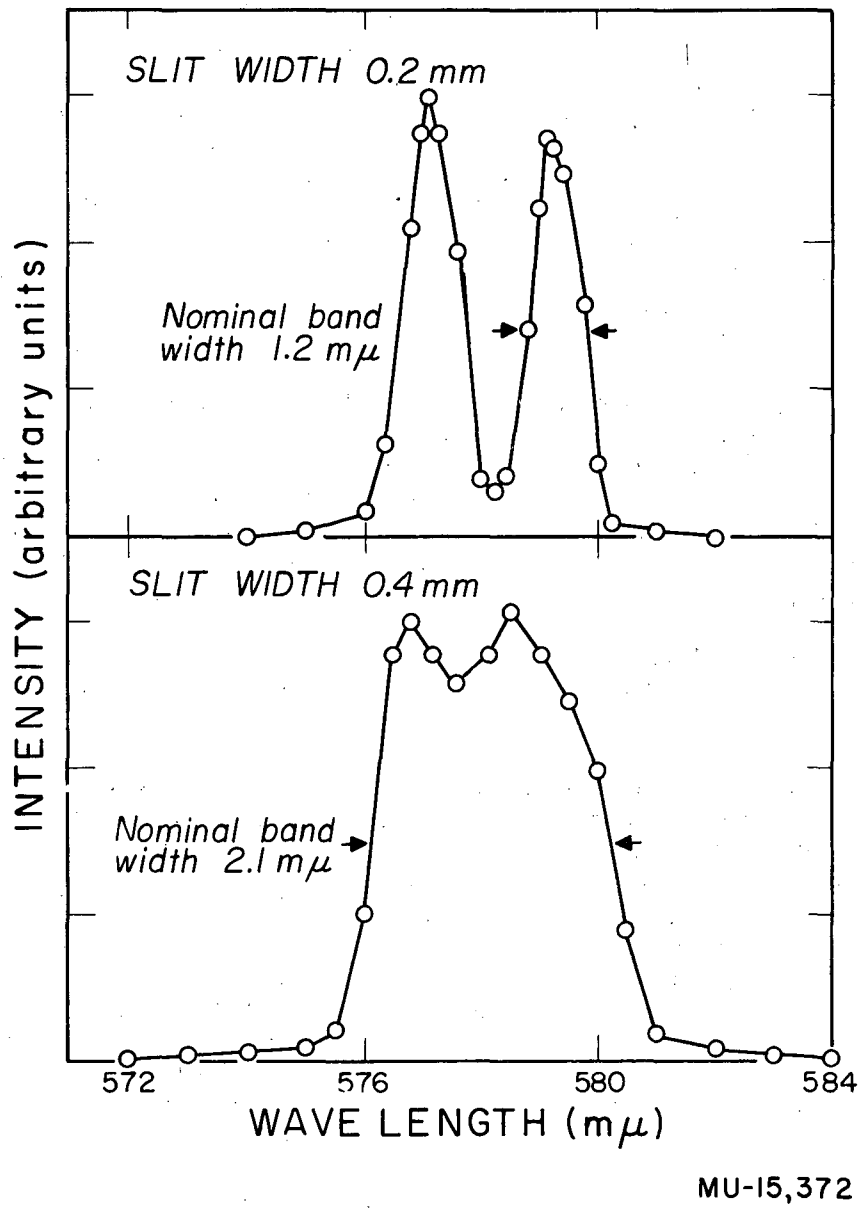

Fig. 7. Spectral purity in monochromator at two different slit widths. Doublet emission lines from Hg at 577 mμ and 579 mμ.

The measurement B was in turn quite inaccurate owing to the large change in the slope of the calibration curve in the region where the image trace was corrected; including planimetry this was estimated to reach 20% in some cases. It was for this reason that the corrected area B was not allowed to exceed 10% of A, in which case the total area did not contribute more than another 2% error to the total area, making a total error of 4% in the measurement.

The total random mass error may then be written as the resultant of these partial errors,

$$\begin{aligned}\delta m &= \sqrt{(\delta\alpha)^2 + (\delta\gamma)^2 + 2(\delta\beta)^2 + (\delta A)^2 + (\delta k)^2 + (\delta \ell)^2} \\ &= \sqrt{(0.01)^2 + (0.02)^2 + 2(0.04)^2 + (0.04)^2 + (0.03)^2 + (0.02)^2} \\ &= 0.01\sqrt{1 + 4 + 32 + 16 + 9 + 4} \\ &= 0.01\sqrt{66}, \text{ or } \pm 8\% \ ,\end{aligned}$$

while the total random error in diameter measurement may be written

$$\begin{aligned}\delta d &= \sqrt{(\delta\beta)^2 + (\delta 1)^2} \\ &= 0.01\sqrt{(0.04)^2 + (0.01)^2} \\ &= 0.01\sqrt{17}, \text{ or } \pm 4\%.\end{aligned}$$

It can be shown that diameter measurements on circular images are accurate to 2% even if the image is traced by a path crossing it at a radial distance from the center of as much as 1/5 the radius. Both this condition and the circularity of each image were checked with a quadrant system on the glass projection screen of the microphotometer. Symmetry in the resulting trace was assumed to indicate circular symmetry in the image extinction.

It should be noted that if no loss of Hb had occurred in the separation, the measurement of total mass was not affected by any size change in the cells after specimen preparation. Size changes in turn are discussed in Part III.

III. EXPERIMENTAL RESULTS

a. Studies on Human Erythrocytes

1. Extinction Coefficient and Absorption Curves

The extinction coefficient for hemoglobin was measured in this study in the following manner. A sample of normal human blood was hemolyzed by 100-fold dilution in distilled water; at the same time the hemoglobin content in a second sample was measured by the Cyan-Methemaglobin method using a Coleman Jr. spectrophotometer. The suspension of diluted blood was allowed to stand for 20 min at room temperature with occasional stirring. The mixture was centrifuged 15 min at 3000 rpm and the clear supernatant decanted. The small amount of white precipitate remaining was discarded. Successive twofold dilutions were made of the supernatant in distilled water. Samples of each were placed in one-cm-path-length quartz cuvettes and readings of optical density at 415 mμ were made on a Beckman D U spectrophotometer. A plot of the data is shown in Fig. 8. The resulting value of extinction coefficient was found to be $6.5 \pm 0.1 \times 105\ \mu g/\mu^2$, and this value was used in all the experiments. Although the relative values within the given population samples are of more concern than are the absolute values, it was nevertheless found (see Table I and the curves) that the mean value of hemoglobin content found microspectrophotometrically in any cell-population distribution was 95 ± 8% of the clinical macrodetermination of its mean value, which is itself about equally inaccurate. The random error is seen to be comparable to that calculated in the last section, while the systematic error is probably due to the specimen conditions.

Normal cells were studied to determine their hemoglobin extinction curves in the wave-length region 385-445 mμ. The shape of these curves provides information about the state of the hemoglobin in the specimen, the effect of monochromator slit width on extinction value, and the extent of inhomogeneity and nonspecific absorption error resulting from the specimen conditions. In these experiments, one series of 13 plates was photographed at intervals of 5 mμ in the above region, using a 1.0-mm slit width on the monochromator, and a second series of eight plates was similarly photographed in the interval 400-440 mμ, using 0.5-mm slit width. The plates were developed and fixed under standard conditions and microphotometer traces were made on the sector steps and on the images of the same cells on each plate. Extinction values above background were than determined for the same point in each cell at each wave length by means of the characteristic curve for that plate.

The resulting extinction curves at points in several cells are shown in Fig. 9. The curves show that little appreciable difference exists between those obtained at slit width 0.5 mm (nominal band width 3mμ) and at 1.0 mm (nominal band width 7 mμ). An absorption curve of oxyhemoglobin in solution is shown for comparison; it is apparent that the shapes of the cellular absorption curves conform very closely to that of oxyhemoglobin in solution

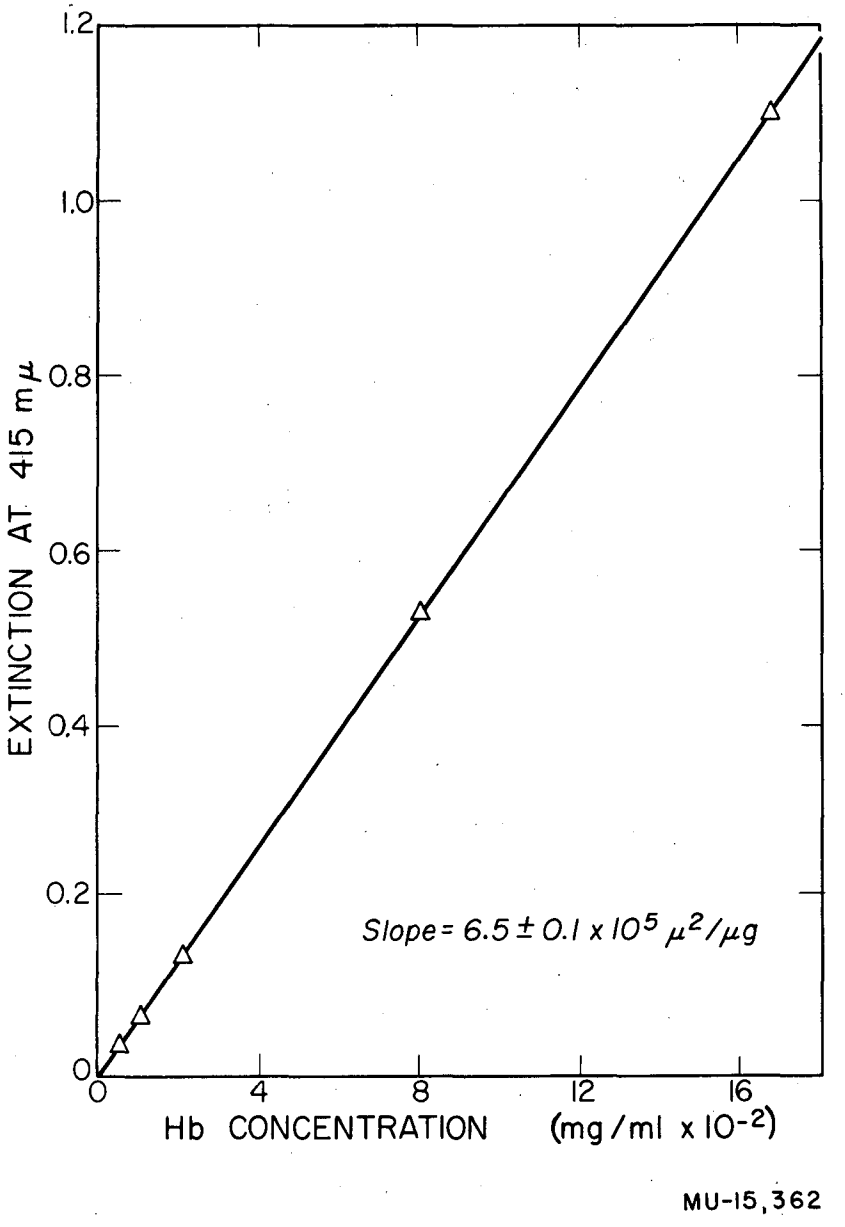

Fig. 8. Determination of extinction coefficient for Hb.

in both cases, while the peak height appears to be uncertain by about 2-4%. It was concluded from these data that absorption readings taken at points in single cells under these conditions were not seriously affected by inhomogeneity or nonspecific absorption, and would provide a valid measure of total hemoglobin mass per unit area at each point; the comparison with the clinical mean values as described above illustrated the degree of agreement.

2. Experimental Material

In this series of experiments, the method described in Part II was used to determine the hemoglobin concentration and total content in individual red cells of blood samples taken from a series of human subjects. Table I lists these with pertinent data for each. Three of the subjects (J, G, O) were normal adult individuals; one of these (J) was sampled twice after an interval of several months. One individual (H) was referred as a possible case of polycythemia vera but after several examinations in the clinic he was tentatively classified as normal, or possibly a case of relative polycythemia of stress. Three of the remaining 4 individuals had been diagnosed as true polycythemics, and they represented 3 increasing states of advancement of the disease (B, M, S). The remaining subject (P) had chronic lymphatic leukemia.* In each case, microspectrographic measurements were made on 100 or more cells; over 1000 measurements were made in all. Diameter and hemoglobin concentrations were determined at the same time for each red cell image, and total Hb content in $\mu\mu g$ (10^{-12}gm) per cell was calculated as discussed in Part II.

Histories (From Clinical Records)

Case H. Male, 37 years of age. Referred as possible P. Vera 8-15-55. Normal Fe plasma concentration. Elevated Fe turn-over of almost twice normal value, (0.62 mg/hr/l) (normal 0.38). In vivo Fe^{59} counting showed a hyperkinetic uptake and release of Fe^{59} by sacral marrow but no splenic or hepatic erythropoiesis. Slight delayed accumulation of Fe^{59} in spleen indicated some sequestration and destruction of erythrocytes in spleen. Considered indicative of a slight hemolytic activity which is completely compensated by increased erythropoiesis. High icteric index; normal total red cell volume during one year (24-27 cc/kg vs normal 24-33) but decreased plasma volume (28-32 cc/kg vs normal 32-45). Florid complexion but no other signs. Never diagnosed as P. vera; some feeling possible polycythemia of stress. 550-cc venesection 12-19-55.

*Thanks are due to Dr. John H. Lawrence, Dr. Myron Pollycove, and the staff of the Donner Clinic for furnishing the clinical data and blood smears.

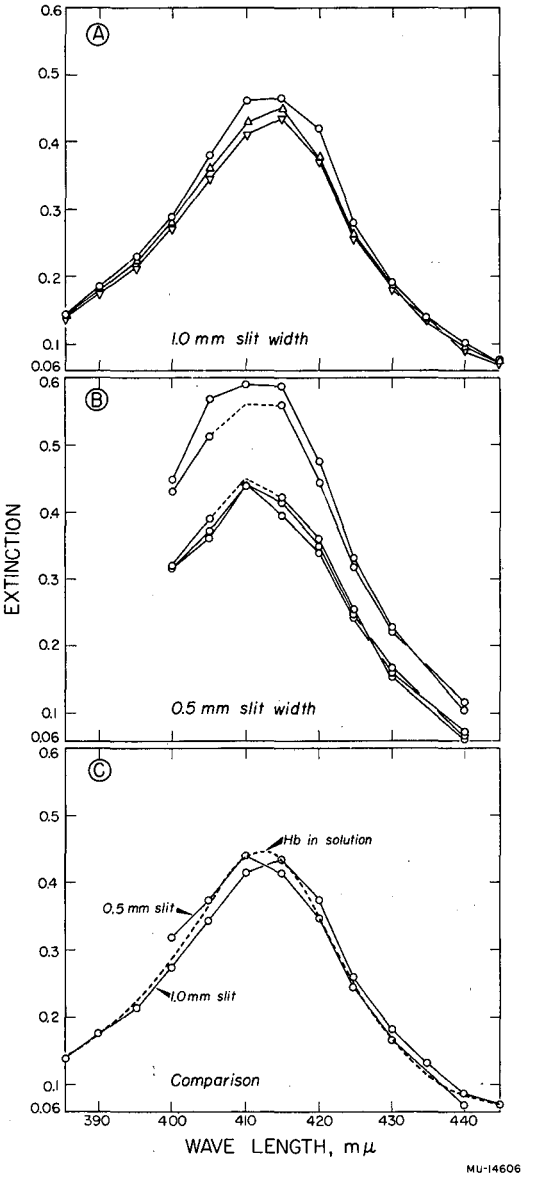

Fig. 9. Hb Absorption curves in single cells.

Table I

Clinical Blood Data

Subject	Sex	Age	Hb Conc	RBC Conc	Hct	MCH	MCHC	MCV	Retic	MCH (micro)	Percent of Clin
J_1 (Normal)	F	27	15.4	5.02	40.0	30.6	38.5	79.6		28.9	95
J_2 (Normal)	F	27	12.3	4.30		28.6				30.0	105
G (Normal)	M	31	15.0	5.09		29.5				28.4	96
H (Normal)	M	37	15.4	4.92	48.5	31.3	31.8	98.5	0.6	30.1	98
O (Normal)	M	33	12.9	4.97		26.0				29.2	112
B (P. V.)	M	60	15.2	5.44	52.6	28.1	28.8	97.0	0.8	29.0	103
M (P. V.)	F	63	19.6	10.35	67.0	18.9	29.2	64.5	1.3	16.7	88
S (P. V.)	M	54	13.5	7.12	49.0	19.8	32.9	68.9	0.4	17.0	86
P (Leuk)	F	65	9.5	3.82	27.5	24.8	34.2	72.0	1.0	22.0	89

Case N. Female, 63 years of age, diagnosis on referral polycythemia vera, 11-13-56. Very high total red cell volume of 42.5 cc/kg (24-33); plasma volume 30.9 cc/kg (32-45) on 11-16-56. Red cell count almost twice normal (10.4 x 10^6/mm^3) at that time; abnormal count first discovered after severe nosebleeds. Microcytosis, hypochromia. Apparently P. vera of several years' duration. Two 500-cc venesections in next two weeks followed by 3 mC P^{32} one week later. By 3-5-57, red cell count was reduced to 7.26 x 10^6/mm^3, while total red cell value had dropped to normal range (30.8 cc/kg), with plasma volume also in low normal region (32.0 cc/kg). No Fe^{59} study recorded. As of 9-17-57, appeared still under control, with red cell count of 5.26 x 10^6/mm; steady improvement had held with no apparent complaint.

Case S. Male, 54 years of age. First referred 9-17-51. Diagnosed at that time as a long-standing rheumatoid arthritis, with recent P. vera. Repeated visits in next 5 years; total of 24.5 mC P^{32} given 4-11-56. Total red cell volume in 1951 61.9 cc/kg; dropped to 43.3 by 4-11-56; plasma volume 25.8 cc/kg in 1951, had risen to 50.9 on 4-11-56.

Fe turnover studies had shown a rapid disappearance of iron from the plasma, with plasma-iron turnover much higher than normal; held to account for the excessive red cell volume if red cell turnover responsible for nearly all this plasma-iron turnover. Later developed myeloid metaplasia or myeloid leukemia; depletion of iron stores has led to a marked iron-deficiency anemia. Bone-marrow function was failing due to progression of the dyscrasia by 1-18-57.

Case P. Female, 65 years of age. Referred 11-19-56; diagnosis on referral chronic lymphatic leukemia. Fe turnover was normal (0.38 vs 0.33-0.43). A nine-day analysis of plasma Fe^{59} showed a total hemoglobin mass of 357 g, with 6.7 g hemoglobin formed daily; mean equilibrium red cell life span was thus 53 days (normal 120-130 days). In vivo Fe^{59} counting showed normal uptake in sacral marrow, slight uptake in liver, none in spleen. In 10 days, normal release from marrow occurred with a considerable secondary accumulation in spleen and a smaller accumulation in liver. It was concluded that the hemoglobin synthesis was normal, there being no compensating increase for the shortened life span of the cells. Accumulation Fe^{59} in the spleen indicated splenic sequestration and destruction of erythrocytes. Total red cell volume on 11-19-56 was 16.1 (normal 24-33); plasma volume was 39.3 (normal 33-45).

Case J. Normal female, 25 years of age. Control.
Case G. Normal male, 30 years of age. Control.
Case O. Normal male, 32 years of age. Control.

The blood specimens were taken from finger puncture in each case. After several drops had freely flowed, 3 or 4 thin smears were made, an even motion usually producing an array of cells in which areas of good spacing between individual cells existed, permitting measurement of background light intensity. No fixation or staining was used; the slides were allowed to dry 20 min in air at room temperature, after which a drop of immersion oil was placed at a suitable region, a cover was slip pressed onto the slide, and the preparation was examined in the microspectrograph at 415 mμ.

In making an exposure the edges of the smears were avoided but an area was always chosen where no clumping, roulade formation, or overlapping of cells had occurred and no distortion was evident. It was usually possible to center the specimen so that an area of blank background could be brought under the path of the sector. Immersion oil between both slide and condenser and cover slip and objective was always used.

A total of 6 to 8 plates was obtained for each case. Exposures were taken at 2 or more areas chosen from each of 2 or 3 slides. Each plate covered a field containing about 30 to 50 cell images. Usually at least 3 good plates were obtained with exposures in the linear range of the calibration curves; the central portions of 3 or 4 such plates were then scanned cell by cell to produce a total of about 100 cells. In the regions of the slides photographed, little crowding of cells had occurred. Further, none of the specimens exhibited any marked poikilocytosis. However, no cell image was scanned if it did not closely approach circularity, nor were images used which were not in good focus.

3. Results

Figure 10 shows 4 scatter diagrams of hemoglobin content plotted against diameter in 500 cells from 5 determinations on subjects J, G, O, and H, and 4 for each cell rather than the calculated total mass, a similar set of correlation coefficients can be obtained for the relationship of mass per unit area and diameter. Scatter diagrams of these quantities are shown in Fig. 11, and these coefficients are also given in Table II. These correlations are seen to be considerably lower than those of mass to diameter; they are negative, and they are significant at the 1-to-5% level; they indicate that only 3 to 30% of the variation in mass per unit area is related to the variation in diameter. In general agreement with the finding of Ambs (1956), there is thus an indication that the two quantities are inversely related, larger cells in general being inclined to show lower densities of hemoglobin per unit area. It should be noted that this quantity cannot be directly related to the concentration of hemoglobin per unit volume, since the thicknesses of the cells were not measured.

An idea of the trend in these relationships can be gained by plotting the median values of mass and of mass per unit area for given diameter intervals. This is illustrated by Fig. 12. From these it is apparent that on the average, the cells of any given diameter class in the populations of B, M, S, and P contain less total hemoglobin and show less density of hemoglobin per μ^2 than those of the same diameter in the normal populations, so that the lowered values of determinations totalling 500 cells on subjects B, M, S, and P. (There were 200 cells in pop. S) (Table I). The mean values of each population are indicated by the quadrants. It is evident in these populations that cells of the same size class may vary in hemoglobin content by as much as 50%, but that a relation between the two quantities exists. If the distributions are analyzed statistically, some characteristics of the populations can be deduced. Using the product-moment formula for coefficient of correlation between the two quantities cell diameter and total Hb content (mass), it was found that diameters

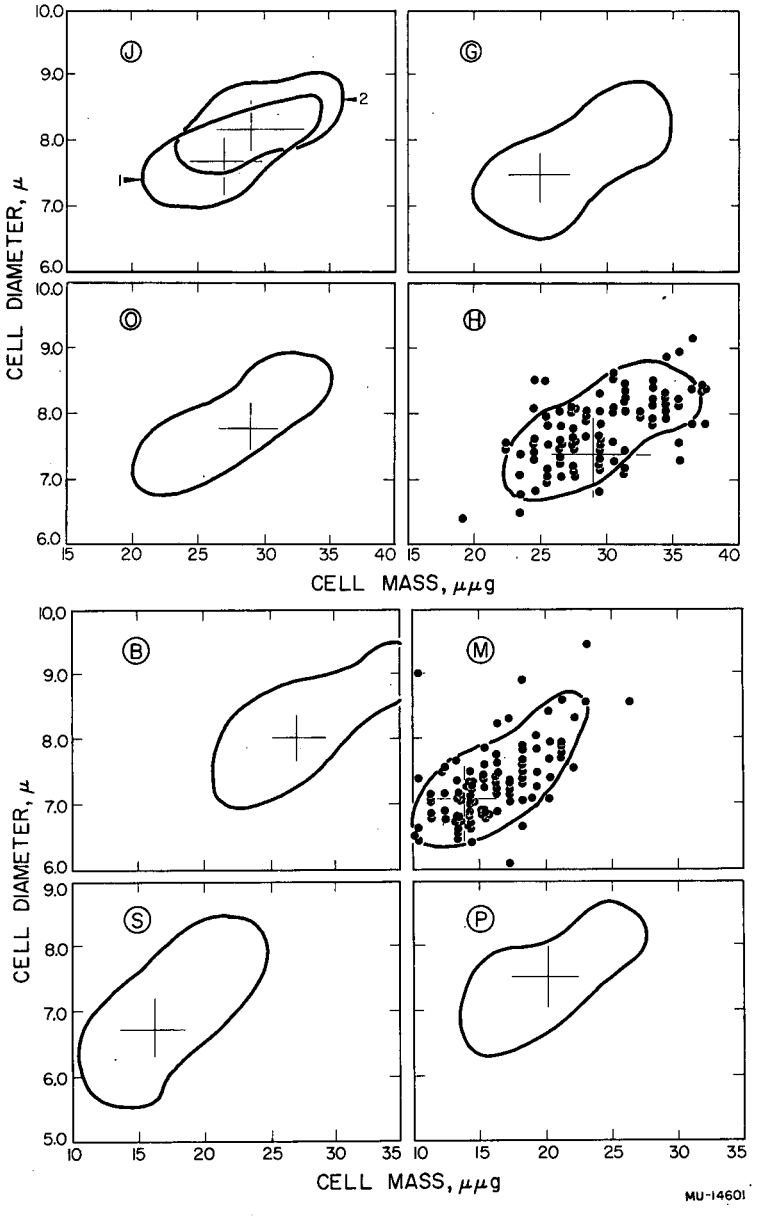

Fig. 10. Scatter diagrams of Hb mass (in μμg) vs red cell diameter (in μ) for humans. The quadrants indicate average values.

Table II

Correlation of Cell Mass and Density with Cell Diameter

Subject	Mass-diam	Percent variance	Signif	Diam-density	Percent variance	Signif
J_1	0.64	41.0	>0.99	-0.25	6.3	<0.95
J_2	0.75	57.0	>0.99	-0.18	3.2	<0.95
G	0.65	42.0	>0.99	-0.41	17.0	>0.99
O	0.77	59.0	>0.99	-0.29	8.3	<0.95
H	0.58	34.0	>0.99	-0.47	22.0	>0.99
B	0.73	53.0	>0.99	-0.79	62.0	>0.99
M	0.53	29.0	>0.99	-0.76	57.0	>0.99
S	0.25	6.1	<0.95	-0.52	27.0	>0.99
P	0.72	52.0	>0.99	-0.20	4.0	<0.95

and Hb masses correlated as shown in Table II. Most of the correlation coefficients fell between 0.5 and 0.8. These values are significant at the 0.1% level for populations of 100, indicating that chance alone could not account for the observed relationship in more than 0.1% of cases. On the other hand, the correlation coefficient may be interpreted by considering that its square is equal to the fraction of the variance, or square of standard deviation, in one variable which is accounted for by its relationship with the other. By this definition it is thus seen that only 30 to 50% of the variation in mass can be explained by its relationship to diameter in any of the distributions.

If the average mass per unit area, which is proportional to the average measured extinction value, is taken total hemoglobin found in the blood counts of these individuals is not due to a subclass of smaller or paler cells within a normal population, but reflects a reduced average content in all the cells, by as much as 1/3. Two tendencies can be seen:

(1) This reduction tends to be quite marked in the cases of the polycythemia and related anemia, illustrated by the positions of curves B, M, and S. In the case of B, the data suggest that the normal average hemoglobin value for the total cell population is maintained only because there exists a considerable proportion of cells with higher-than-normal diameter; all the size classes of cells already tend to be slightly lower in Hb content in this mild case than do their counterparts in a normal population.

(2) The tendency of smaller cells to show a slightly higher density of hemoglobin than the other cells, which is evident in normal populations, almost disappears in the diseased populations.

These considerations also apply to the cell population of the leukemia case P.

The scatter diagrams of mass versus diameter in Fig. 10 may be regarded as probability distributions in which the values of probability would be heights on a third axis perpendicular to those of both mass and diameter. These probability values are proportional to the density of points per unit area on the scatter diagram on the m-d plane in the neighborhood of a given value of m and d. If the surface so generated is projected onto a plane through the m axis perpendicular to the m-d plane, a frequency-distribution curve of masses results, while the same holds for diameters in the plane perpendicular to the m-d plane through the d axis. Figure 13 shows the resulting frequency distributions of cell diameters for cases J, G, H, and O, and B, M, S, and P. These are seen to be the Price-Jones curves of the given populations.

Curves depicting the distribution of total cellular hemoglobin mass in the populations can now be constructed, analogous to the Price-Jones curves; the information contained in them differs from that in Price-Jones curves owing to the looseness of correlation between mass and diameter, and this information cannot be derived from the latter curves. Figure 14 shows these hemoglobin mass distributions for the same populations.

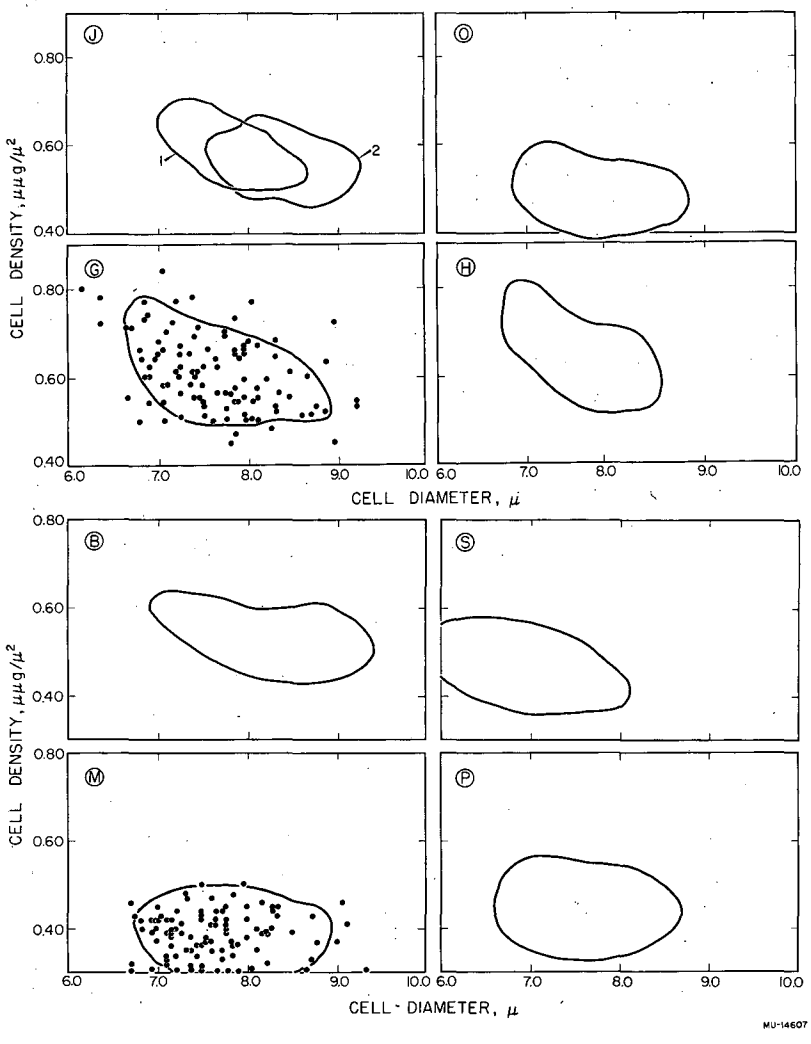

Fig. 11. Scatter diagrams of Hb density in $\mu\mu g/\mu^2$ vs red cell diameter in humans.

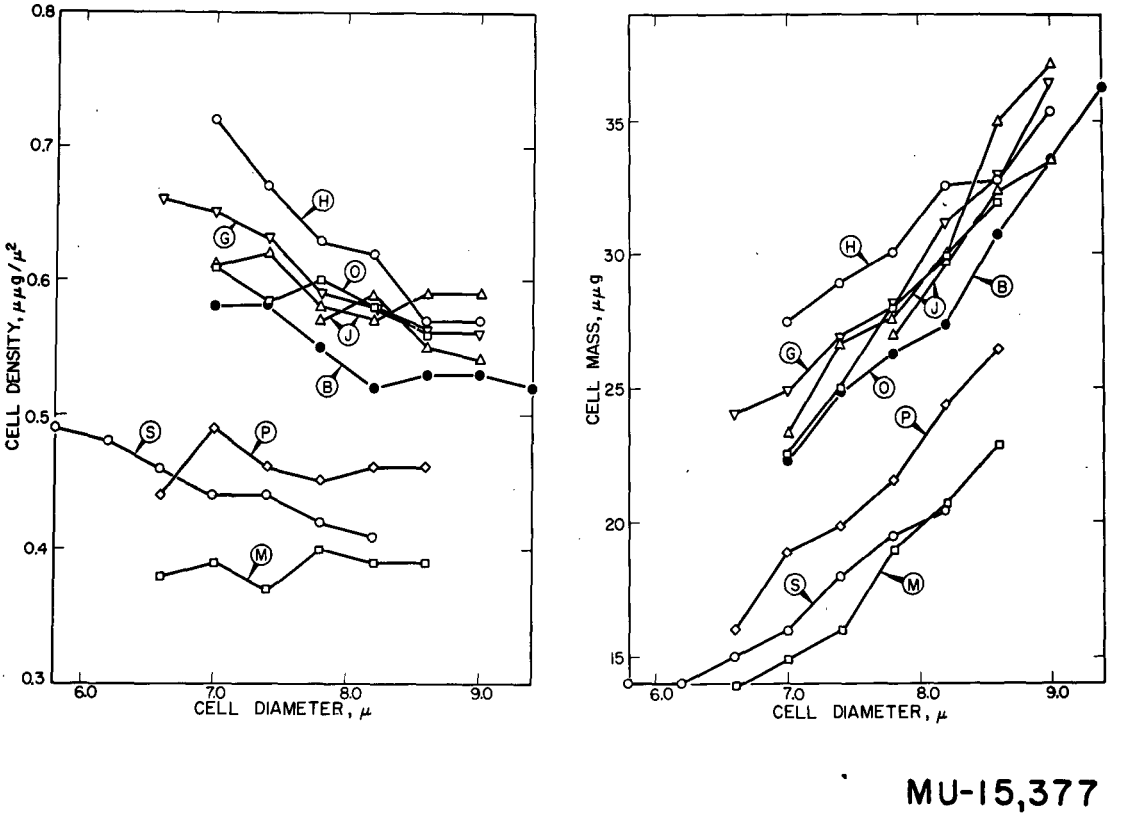

Fig. 12. Median values of Hb content and Hb density vs size in human red cell populations.

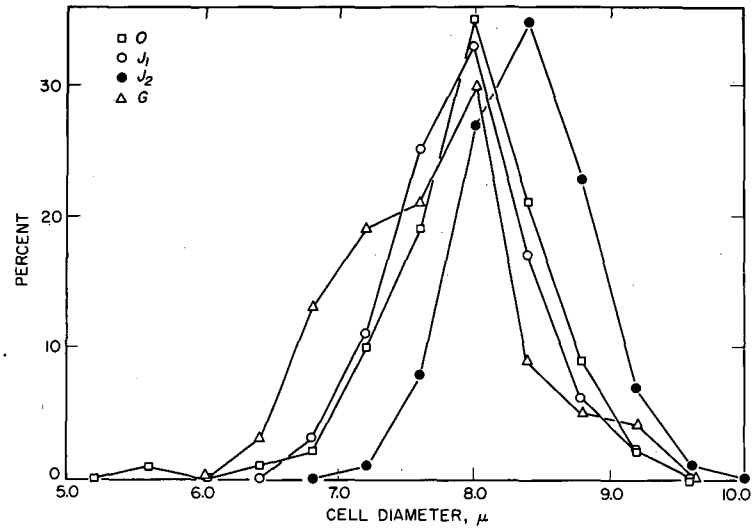

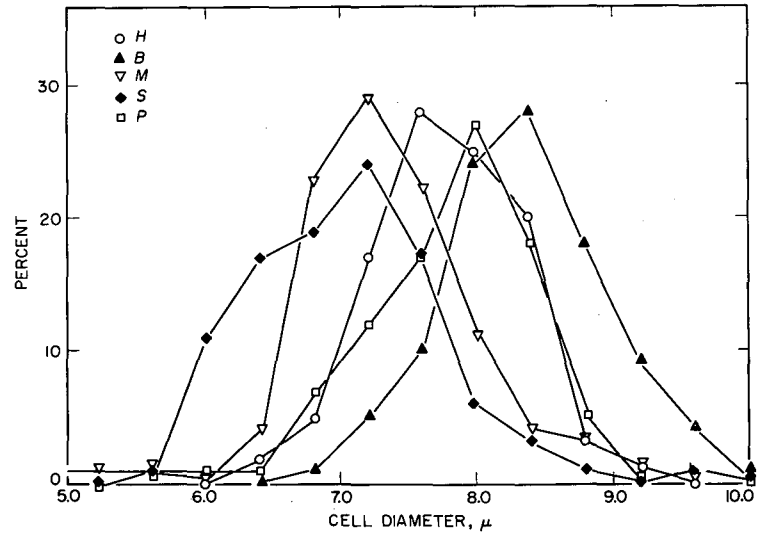

MU-15,378

Fig. 13. Frequency distributions of red cell diameters in the human cell populations.

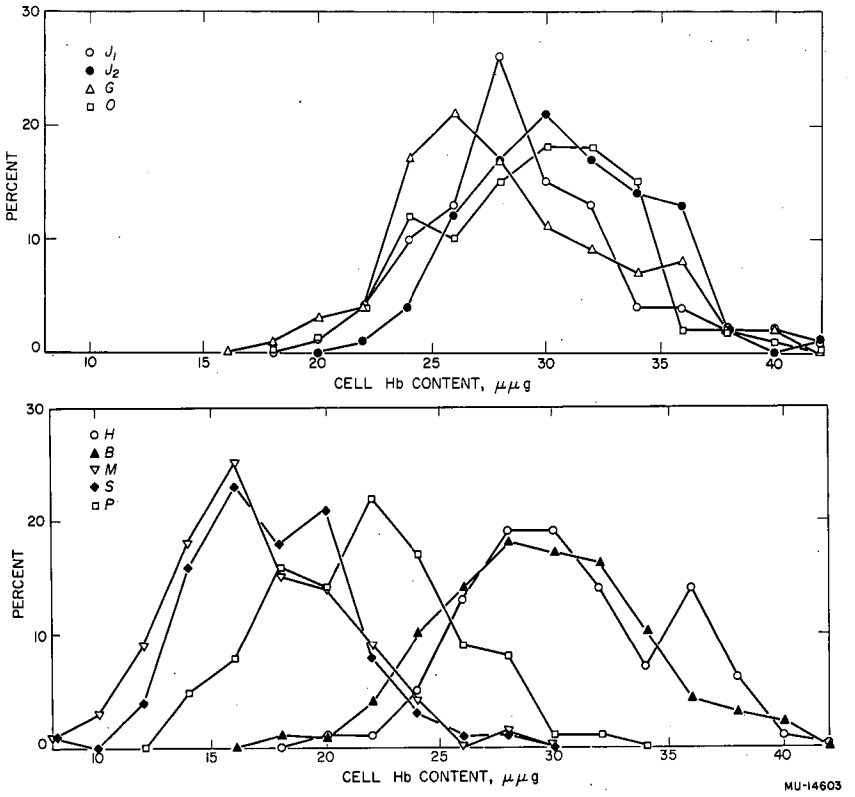

Fig. 14. Frequency distributions of red cell Hb content in the human cell populations.

Figure 13 shows that the frequency distributions of cell diameters are Guassian, or normal, distributions for all the populations. Further, the median values of diameter apparently do not greatly differ between the groups except in the distributions of M and S, where the medians are near 7.0 μ, whereas the other medians cluster around the value 7.8 ± 0.3. This is brought out more clearly by the use of probit diagrams. If a normal distribution is plotted cumulatively in terms of the number of probits, or standard deviation units, by which each sub-class differs from the mean of that distribution (plus 5 probit units, here neglected) a straight line results. The same thing is accomplished graphically by transforming the scale of cumulative percentage of cell numbers on one axis to be linear in terms of standard deviation units, as is done on probability paper. Figures 15 and 16 illustrate the probability diagrams of the populations grouped into the sub-class intervals shown with respect to both diameter and Hb mass. It is seen that most of the diameter distributions are well fitted by normal approximations, although populations G, H, M, and S are suggestive of a slight alteration in number of largest and smallest cells in terms of their own population distributions. Thus G shows twice as many and H half as many cells as expected above the 90% level at the large-diameter end, while M and S both show half as many cells as expected below the 10% level at the small-diameter end. In populations of this size, however, these differences are not great enough to be significant at the 95% confidence limits, i.e., these differences from a normal distribution could occur by chance alone about 5% of the time in groups of this size. The 95% limits are marked on one distribution.

In the case of total cellular hemoglobin mass, a somewhat different situation exists. Figure 16 shows that considerable differences exist in the median values of hemoglobin content between groups of J, G, O, H, and B and that of M, S, and P, as was already known from the macrodeterminations. In addition, certain other regularities suggest that further interpretations of population behavior may be made.

a. The points denoting cumulative class intervals are closely fitted by normal curves (straight lines) for the lower half of the mass distribution, but a curvature appears at about the median (50%) level in all five distributions of J, G, O, and H, suggesting a consistent skewness in the distributions. The curves are plotted between the upper and lower 2% limits; i.e., better than 95% of the observed values are located between these limits. The observed curvatures correspond to a tail of relatively many higher-mass cells in these populations, there being, for example, about twice as many cells as expected at the 32-μμg level and above, as a normal distribution and standard deviation based on the rest of the population would predict. This is particularly evident in the cases of H and G, which show 4 times the expected numbers at 32 and 34 μμg and exhibit a definite bimodality in the frequency polygons of Fig. 14, suggesting a second population with median value 36 μμg in addition to the main one at 29 μμg. These differences fall between the 99% and 95% confidence limit and are in the same direction for all 5 populations.

b. The closeness of fit to the points in the first half of the distributions suggests the existence of a "backbone" curve, the slope of which is identical in all the populations of J, G, O, and H. This slope is a measure of the standard

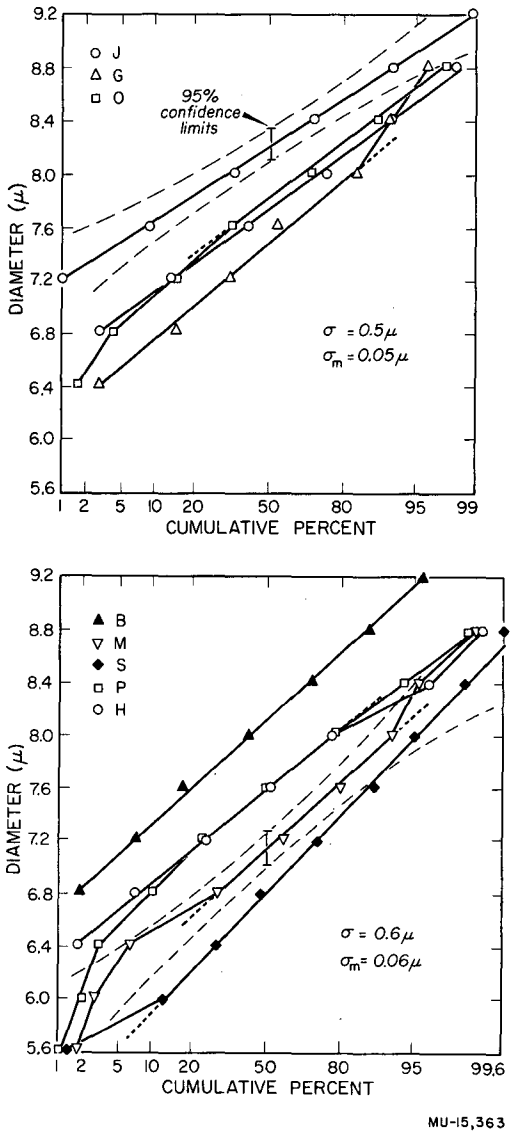

Fig. 15a. Probit diagrams of red cell diameter in human cell populations. Cases J, G, O.

15b. Probit diagrams of red cell diameter in human cell populations. Cases B, M, S, P, H.

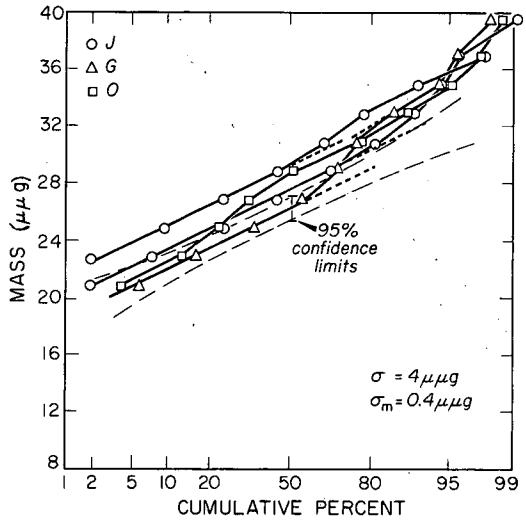

(a)

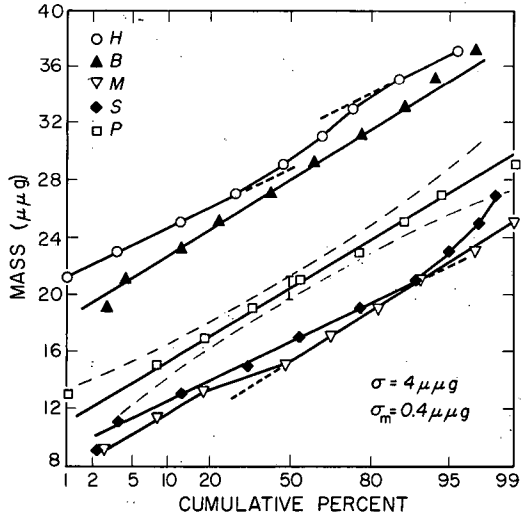

(b)

Fig. 16a. Probit diagrams of red cell Hb mass in human cell populations. Cases J, G, and O.

16b. Probit diagrams of red cell Hb mass in human cell populations. Cases H, B, M, S, and P.

deviation of a normally distributed population with the given median value.

c. In the cases B, M, S, and P, no such upward curvature is observed except in S, where, however, it is small and is not significant at the 95% level. Conversely, in case M a truncation is suggested at the lower end, signifying a slight reduction in the relative number of small-mass cells, but this deviation is also insignificant at the 95% level. The slopes of curves B, M, and P are increased and are very nearly the same; this suggests that these populations have a somewhat greater standard deviation and are spread into a larger range.

4. Discussion

Measurements of hemoglobin content and concentration in erythrocytes, as usually determined, are average values for very large numbers of cells. Under this circumstance the characteristic structure of the population cannot be investigated. A knowledge of the relative numbers of cells with values differing from the mean value in either direction, the range of this variation, the shape of the distribution and the existence of discrete subclasses would, however, contribute toward further understanding of the processes which produce the populations. The microabsorption measurements discussed here are an attempt to develop such a description, and some tentative interpretations may be drawn from them. The differences between the populations resulting from normal hemopoiesis and those in the disease states are not striking, and since the ages of individuals differed in the groups, it cannot be ruled out as a factor in the differences. However, there are distinctions, which may be summarized briefly as follows.

a. There is a lowered Hb content and Hb density per unit area in the cells of the population as a whole in these diseased populations, and it is true of all cell sizes relative to their normal counterparts.

b. There is a tendency for the smallest cells in the normal populations to exhibit the highest mass per unit area, which is not so apparent in the populations from the diseased individuals.

c. There is some indication of a skewness, i.e., a tail or even a subpopulation, of high-mass cells in the normal populations, which is not evident in the others.

Some possible interpretations will now be discussed.

a. The lowered Hb content in all the cells of populations M, S, and, to a slight degree, in B undoubtedly follows from the higher demand on the iron stores caused by increased red cell production. In the case of population P, the shortened life span inferred from the tracer measurement, which was not compensated by any increase in production, would seem to indicate that the high rate of loss of red cells was accompanied by an iron deficiency which simply prevented the increase. In the populations of M and S, the average

size of the cells is also decreased, but even in those cells which are of normal size, the Hb synthesis has been depressed enough to produce a lower Hb total mass than in normal cells of the same diameter range. This relative deficiency at all size levels is seen to be quantitatively less marked in population P, where the normal production rate has apparently resulted in normal-sized cells all of which again contain less Hb than normal cells of the same size range, but here the total amount of Hb per cell in each size class is nevertheless higher than in the cases of M and S. Since the mean corpuscular volumes of M and S are depressed slightly more than is that of P (Table I), while the mean corpuscular concentration of Hb is almost normal in all three, the mean cell thicknesses of M and S must also be less than that of P. Since thickness and therefore volume could not be measured in the individual cells, it was not possible to determine whether this was true for each size range. However, the average Hb mass per unit area was found to be lower for each size range in P, S, and M than in the correspondingly sized normal cells. Whether this resulted from a normal concentration but a smaller thickness, or both somewhat smaller, or from a normal thickness and lower concentration, could not be decided.

The question of the constancy of Hb concentration in all sizes of cells has been discussed by many authors, among them Ponder (1948), who discusses the relative constancy of Hb concentration among many animal species with widely differing cell diameters and volumes; and Wintrobe (1952), who concludes from the work of several other authors that cellular Hb concentration remains constant, for example, in the macrocytosis of pernicious anemia, the increase in total cell content being directly proportional to the increase in cell volume rather than to an absolute hyperchromia. Perutz (1948), in discussing the results of x-ray scattering experiments by Dervichian and Magnant (1947) on red cells, points out that the mean distance between Hb molecules found, together with the known lack of birefringence in intact red cells and the known asymmetry of the Hb molecule, argues that the molecules are freely rotating in a close-packed lattice. To pack the greatest number of such molecules and still allow freedom of rotation, an intermolecular distance at least equal to the effective molecular diameter would be required, and the known dimensions of the Hb molecule fit this condition as found in the scattering studies. This condition then leads to a concentration of 34%, which is probably the optimum value compatible with both maximum oxygen-carrying capacity and highest speed of reaction and diffusion of oxygen through the cell.

It thus seems quite possible that a thickness variation and not one of concentration must be responsible for the range of Hb densities encountered in cells of different diameters under different conditions; the variability of mean corpuscular Hb concentration as measured clinically may be due more to differences in cellular permeability to water in packing of cells after centrifugation than to intracellular changes in the in vivo populations. In any case, in dried smears it is likely that the main portion of water remaining inside the cells is only that bound to the Hb, so that the concentration of Hb would tend to be high and constant in all the cells and thickness differences would be mainly responsible for the different values of Hb per unit area, whatever had been the case in the cell originally.

In this connection, some considerations on shape changes in dried red cells are here presented. Ponder (1948) tabulates average dimensions of normal human red cells in plasma as depicted in Fig. 17. As a check on the validity of the absorption images, and to provide some rough indication of shape changes in the cells of the dried smears, a calculation was made of the transmission through the absorption image which would result from a cell with the above shape factors. This image trace is illustrated in comparison to two experimentally obtained traces of normal cells, using the same value of mean corpuscular Hb concentration in the calculation as was determined by measuring the hematocrit of the total sample. The relationships are shown in Fig. 18. If the cell shape given by Ponder is used, Curve A results, while the same total amount of Hb redistributed in a disc of the same diameter produces Curve B.

Ponder states that shrinkage occurs in dried blood films which results in a decrease of 8 to 16% in mean cell diameter compared to the values in plasma, i.e., the mean value for man in plasma is 8.5 μ, while in dried smears it is 7.3 to 7.5μ according to his own, and about 7.5 to 7.8 μ in other determinations, most of which agree to within about 0.3μ (Ponder and Saslow, 1929). Upon reducing all the dimensions of a biconcave disc by 15%, a volume loss of 40% occurs; the actual value given by Ponder and Millar (1924) is 35 to 45%. If it is assumed that all dimensions are reduced by 15% but that the total amount per cell remains the same, Curves C and D result for biconcave discs and flat discs respectively. It is seen that peak extinction values of well over 1.00 (peak T over 95% on plate) result in Curve C, while in Curve D the extinction values approach 0.50. None of the cell images measured exhibited values as high as that of C; they seldom reached the level of D in the flatter forms.

In addition the total amounts of Hb per cell remained about the same, for the mean values of cellular Hb content determined microspectrophotometrically were within the range of 0.95 ± 0.08 of the clinical mean values in all the normal cases, as before stated. This quantity is of course not influenced by shape changes if no leakage has occurred in preparation. The mean values of diameter found were larger than his figure of 7.3 to 7.5μ, being 7.8 ± 0.2μ. The probability of this mean value's occurring by chance alone in a population of 500 cells is less than 1%. In view of these observations, it is concluded that shrinkage effects, which affect diameter measurement but of which total mass measurements are independent, did not produce diameter reductions as large as Ponder's values predict in these studies. Variations in individual size and content are of course the very factors under consideration and they do not allow a precise estimate of the true degree of such shrinkage, but (a) the observed high mean diameters, (b) the expected average content, and (c) the extinction values--which resembled Curves A and B more than Curves C and D--together suggest that such shrinkage in diameter was probably near Ponder's lower limit of 8% at least in most of these preparations. It would be difficult to determine whether such shrinkage had occurred uniformly in all directions, but the results suggest that the main change was in thickness. To know whether the cells would shrink differently according to their size would be essential to a critical evaluation of the size-mass relationships discussed here.

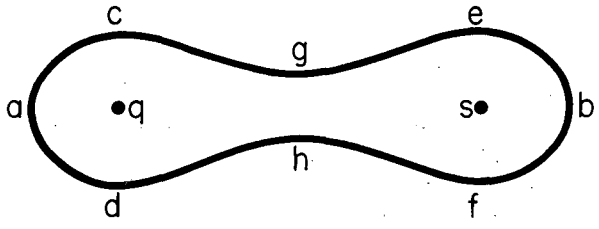

Quantity	Man	Rabbit
ab	8.5μ	7.3μ
(cd+ef)/2	2.4μ	1.7μ
gh	1.0μ	1.0μ
(qa+sb)/2	1.3μ	1.1μ
vol	87μ^3	57μ^3
σ (diam)	0.41	0.37
σ (cd)	0.13	0.13
diam-cd correlation	0.39	0.44

MU-15,365

Fig. 17. Average dimensions of normal red cells in plasma (Ponder).

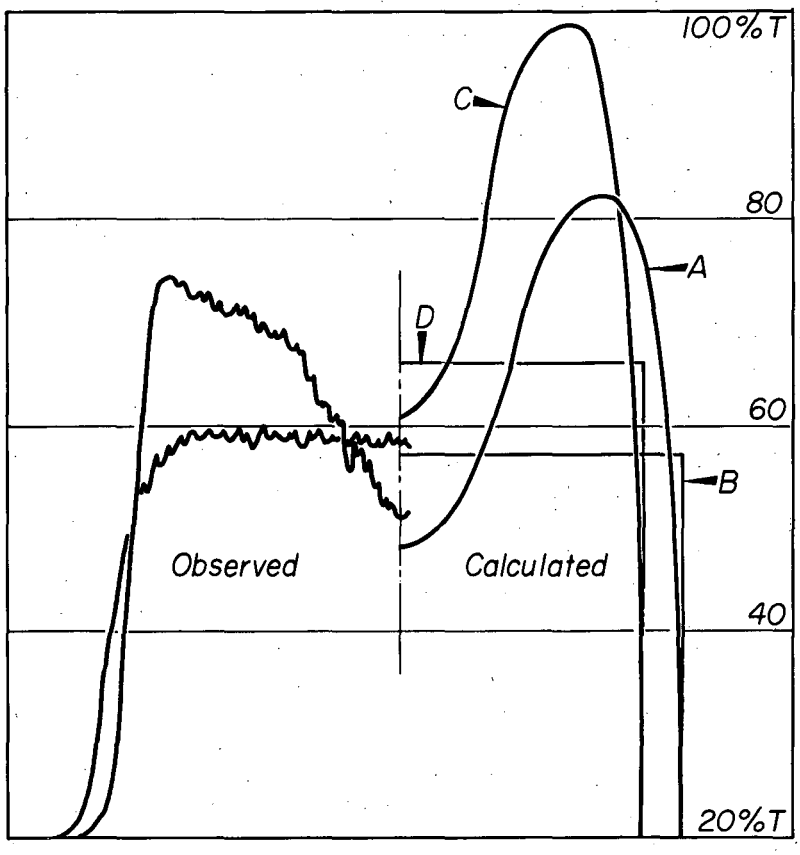

Fig. 18. Absorption curves calculated from Figure 17, compared with representative observed traces.

b. The correlation of mass per unit area to cell diameter is low. However, there does appear to be an inverse relation of density to size, which is slightly more pronounced in the populations J, G, O, and H as a whole than in those of B, M, S, and P (Ambs, 1956). Whether this is due to a different behavior of the cell populations physiologically, or is a shrinkage effect which is lower in the smaller cells of a population with low Hb content throughout, or perhaps is even influenced by pH variations in the blood of the different subjects, cannot be determined by the data. Since, however, the youngest mature red cells, the reticulocytes, are known to be larger than the average of any population (Persons, 1929) and to accumulate at the top of a column of centrifuged cells (Borum, Figueroa, and Perry, 1957) (see Part IIIb), the possibility may be suggested that the smaller, denser cells usually represent the older members of the distribution, and that in the M, S, and P populations at least two possible mechanisms might be responsible for the difference in the trend between the two population series.

First, all red cells may lose Hb with age, either actually or functionally, and many of the older cells in these latter populations may not retain as much Hb as do their counterparts in the undisturbed populations; they may become more fragile and be subject to more leakage, either uniformly or during part of their lifetime. Such cells might either disappear after a shorter life span than in the other populations [or perhaps lose more Hb while young]. Second, whereas young peripheral cells in normal populations may carry on a small additional metabolism and Hb synthesis (Nizet and Lambert, 1953; Austoni, 1954) during at least the early portion of their lifetime in the circulation, and thus might partially compensate for such an approaching Hb loss occurring in all cells and for the size reduction of aging by slightly increasing their Hb content, this metabolic capacity might be impaired in many cells of the abnormal populations. Though these possibilities are intriguing, it must be admitted that they cannot be proven by the data. Further experiments combining the microabsorption method with the method of microradioautography are necessary towards establishing or disproving such hypotheses, and a further study using this combined approach is planned.

c. The deviation from straight-line plots on the probability scale of all the populations J, G, O, and H is an indication of distributions which may either be skewed toward higher-than-normal numbers of high-mass cells as in J and O, or may even contain distinct subgroups of high-mass cells, as is suggested in G and H. The degree of curvature in any distribution is of borderline significance, as is indicated by the 95% confidence interval giving the limits of random variation about the theoretical straight line which is inserted for one curve. The fact that it occurs in the same way to some degree in all five plots does, however, strengthen the possibility of its significance. Some further considerations are given below which tend to support this view.

If the scatter diagram is plotted on log-log paper, a regression line of log m on log d may be graphically fitted to the medians of the subclasses, and a second regression line of log d on log m may also be fitted. (The correlation coefficient is given by the square root of the ratio of the slopes of these lines.) For one scatter diagram of population J the regression equation was found to be

$m = 0.32\ d^{2.2}$, and a correlation coefficient was found of 0.94. If now the probability plot of this and the other populations is transformed to a log m scale as in Fig. 19, the skewness is seen to have lessened or even disappeared. If, further, the experimentally observed cumulative per cent diameter distribution for J_1 is now transformed into a mass distribution by the above regression equation and plotted on the same graph, it is seen that the observed mass distribution for J_1 is closely fitted.

This would lead one to assume that the skewness in the population probit curves of mass could result simply from a relation of mass to diameter which is about what would be expected for disc-like objects of thickness around 1.4μ and concentration about 34% Hb, varying normally over the observed diameter range.

The questions then arise: (1) What would account for the increase in Hb area density at small diameters in the skewed populations J, G, O, and H, and (2) What might account for the absence of both skewness and density increase in populations B, M, S, and P?

In view of the smallness of the samples and the limitations on the data the same strong qualifications must apply to any interpretation, making the resulting possibilities little more than speculations. One might nevertheless hypothesize that in the undisturbed populations the same Hb loss with age, now combined with better retention or compensatory increase in Hb mass, keeps more of the smaller-diameter cells in agreement with this approximate relation, while less retention or less increase in the other populations leads to a nonskewed or straight-line probit plot. Alternatively put, this would imply that (a) although the older smaller cells in the disturbed populations have become denser as they decreased in size, they still have lost more Hb during their lifetime than have their counterparts in the undisturbed populations; or else, that (b) they might have continued to synthesize a small amount of additional Hb after entering the peripheral population, but instead for some reason lacked the capacity to do so and therefore could not partially compensate for the Hb loss due to aging which was common to all.

If all the populations are similarly plotted on log m-probit scales, the "undisturbed" populations H, G, and O and J, are now more linear and show very similar slopes (Fig. 19), while a departure from this same slope, indicated by dotted lines, does indeed appear at the low-mass end of the log curves for B, M, and P, while the log curve for S is now all at the higher slope. In the low-mass region, a transformation from diameters to masses by a power law as described above would fail, many more of the cells being of lower mass than one would predict from the average mass-diameter relationship of the rest of the population. It might be argued that such a difference in population behavior as seen in Fig. 19 might be due to alterations in the pattern of release of young cells into the circulating population, as, for example, a premature release of incompletely differentiated cells of lower Hb content, truncating the high ends of the Hb distribution curves. However, this seems unlikely for two reasons: (a) young cells would be likely to have larger diameters and masses than those of the main population; and (b) the slopes of the log mass curves of B, M, S, and P would then be expected to

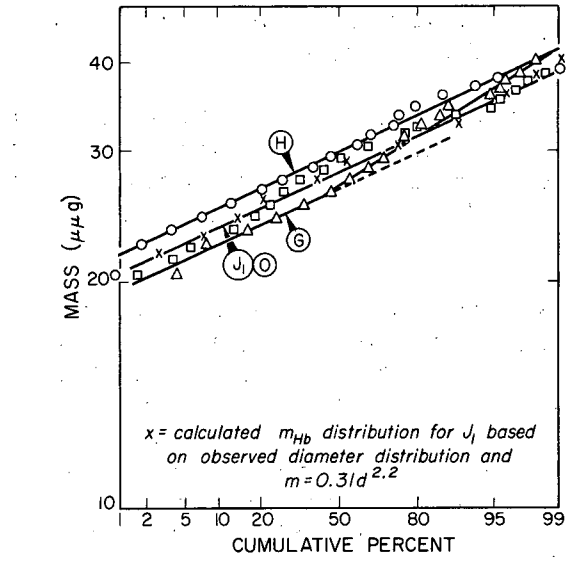

(a)

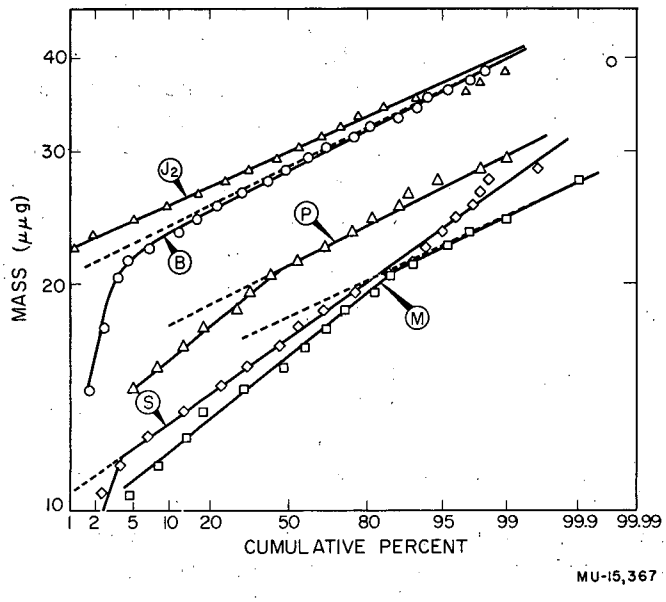

(b)

Fig. 19a. Log probit diagrams of red cell Hb mass. Cases J, G, O, and H.

19b. Log probit diagrams of red cell Hb mass. Cases B, M, S, and P (and J_2).

differ from those of J, G, O, and H at the high-mass end rather than at the low, while their slopes at high-mass range are instead similar. The fact that the differences seem to appear here at both the low end of the mass distributions (Fig. 19), and at the lower-diameter end of the density-vs-diameter plots as a less increased density (Fig. 12), therefore suggests that they would be due to a difference in aging behavior rather than to an altered mode of release of new cells. Some results which will be given in the next section also tend to support this hypothesis.

b. Studies on Erythrocytes of Normal and Irradiated Rabbits

1. Material and Methods

In this series of experiments, the microabsorption method of Part II was used to study the behavior of Hb concentration and content in the individual red cells of the peripheral blood of x-irradiated and normal rabbits. The same procedures were followed as discussed in III, Part a. Rabbits from the standard animal-colony stock of this laboratory were used, and the animals were kept on a regular laboratory feed throughout the period of study. Full-grown rabbits weighing between 3 and 4 kg were used and blood samples were taken from a total of 6 animals. Table III shows the conditions and sequence of the determinations. Five of the animals were irradiated in the sublethal range, while one was kept as control and used for an experiment with centrifuged blood. Cell-population distributions were studied in the microspectrograph as indicated in Table III. The samples used for analysis were chosen from 3 of the animals at the times indicated. A total of 10 samples of about 100 cells each were measured, more than 1000 cells being measured in all. No attempt was made to obtain complete sequence of samples on all the animals, owing to the amount of time required for the determinations. Instead, specimens from one animal were analyzed twice, once just prior to irradiation and once at 2 days post-irradiation; death occurred for this animal on the third day. Seven other analyses were done on samples from two of the other animals; these were taken just before irradiation and at two and three times thereafter during the period of marrow depression and regeneration. One animal died the day after the third sampling at 23 days, while the other survived. One other animal was sampled as a control, and a cell-population analysis was made on the top and bottom layers of a column of centrifuged blood taken from this animal. Each animal was weighed whenever a sample was taken. The 3 irradiated animals upon which cell-population analysis was carried out all served as their own controls by the analysis of the samples taken just prior to irradiation. All 4 of these distributions were found to agree quite closely both among themselves and with the macrodeterminations of average cellular Hb content taken on the other 2 animals. These data will be discussed in the following section.

The technique of irradiation was as follows. After weighing and blood-sampling by ear puncture, the animal was confined in a ventilated irradiation cage of masonite, which was placed on a rotating turntable centered in the axis of the x-ray beam. The distance from target to the center of the animal was 80 cm, at which point the dose rate measured in air with a Victoreen rate meter was 28 r/min. The dose rate at the ends of the irradiation cage was found to be

Table III

Rabbit Irradiation and Sampling Sequence

Animal Number	Dose	Sex	0 Days	2 Days	11 Days	23 Days	44 Days	77 Days
1	600r	M	MCH 18.8 Wt 3.68 kg		24.30 3.29	←(7 %Retic) 3.20		
2	600r	M	* Wt 3.41 kg	* 3.29	Died 3 days			
5	600r	M	* Wt 3.82 kg		* 3.39	* 3.30	* 3.40	3.71
6	600r	F	* Wt 3.07 kg		* 2.76	* 2.72	Died 24 days	
7	Control	M	* Wt 3.56 kg	MCH 20.6	Centrif.			
11	600r	F	MCH 20.5 Wt 3.70 kg		22.10 3.51	←(5% Retic) 3.44		

*Cell-population analysis on sample.

85% of that at the center at this distance. Each exposure was 21.4 min in length, to give a total of 600r at the center point, and the beam intensity was monitored throughout the exposure by placing the ion chamber at an off-axis point and checking the rate-meter reading for constancy. A Phillips x-ray unit was used at 230 kv(p) energy, 15 ma tube current, and 0.5 mm Cu + 1.0 Al filtration. With these factors the mid-line dose to the animals was about 700 r, a depth-dose fall-off at 5 cm from the upper surface of the animal of about 20% applying to a skin dose about 50% higher than the mid-line air dose (Bond et al., 1956). The animals were returned to their cages immediately after irradiation.

2. Results

Table III gives the weights of animals at the time of each sampling. It is seen that a weight loss of 11% had occurred for rabbit No. 5 and 10% for No. 6 on the 11th day, after which No. 6 dropped further in weight to 88% of the control value by the 23rd day, while No. 5 decreased further, then began to regain weight, reaching 87% of control weight at 23 days and rising to 97% at 44 days. This degree of weight loss is about that to be expected in rabbits for a dose in this region.

Figure 20 illustrates the scatter diagrams of Hb content vs diameter in the cell population of rabbit No. 2 at 2 times; pre-irradiation (0 days) and at 2 days after irradiation. This animal died at 3 days. Figure 20 also shows the same plots for rabbit No. 6 at 0 days, 11 days, and 23 days, after which this animal also died, at 24 days. The figure finally shows the same plots for rabbit No. 5 at 0 days, 11 days, 23 days, and 44 days; this animal was still alive at 90 days.

The degree of correlation between diameter and Hb content in the control populations is seen to be comparable to that of the human populations discussed in the last section; correlation coefficients for the 2 quantities are given in Table IV together with their levels of significance. Table IV also lists the correlation coefficient of mass per unit area with diameter, and Fig. 21 illustrates this relation. The inverse relationship is again slight but evident, but the correlation coefficients and the degree of scatter in the plots are seen to differ considerably between the irradiated and nonirradiated animal.

If median values of both mass and density for given diameter intervals are plotted against diameter as before, the trend of this relation is again illustrated, the plots now representing different times for the same animal. This is shown in Fig. 22, which shows the mass-diameter relation at the different times after irradiation for each of the 3 animals, and Fig. 23, which shows the relation of mass per unit area to diameter in the same way. The points in these plots have again been connected instead of drawing regression lines in order to illustrate a tendency toward curvature in the scatter plots, as was also the case with the human data.

As in the human data, it is again apparent that the larger cells are on the average a little less dense than the smaller ones. However, both the high mass-diameter correlation and these plots indicate that the large cells

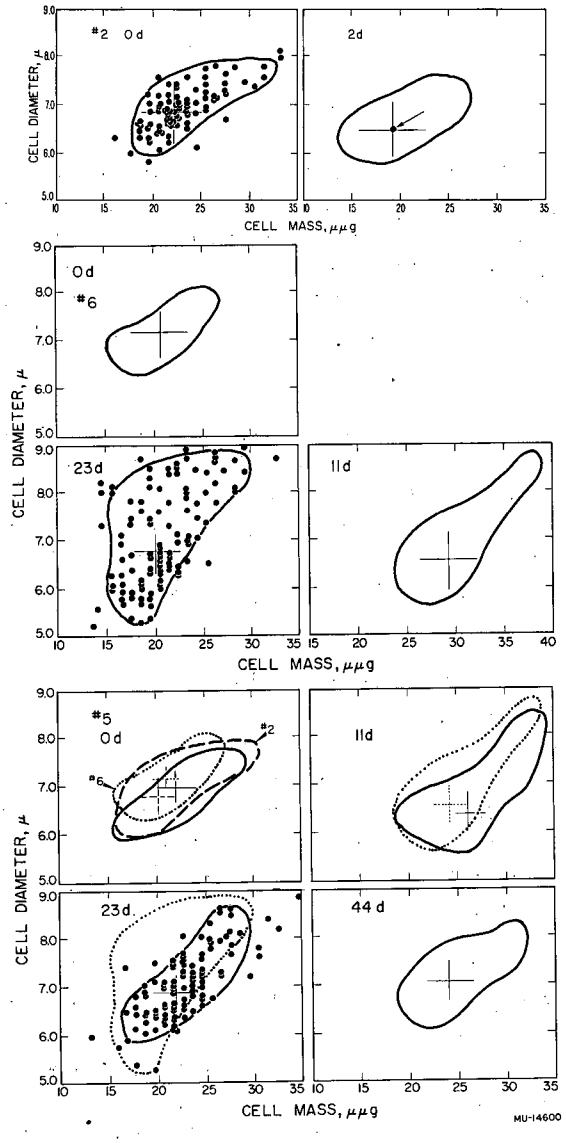

Fig. 20. Scatter diagrams of cellular Hb mass vs cell diameter in rabbit red cells of three animals, at different times following 600r total-body X-radiation.

Table IV

Correlation of Cell Mass and Density with Cell Diameter

Animal	Time	Mass-diam	Percent variance	Signif	Diam-density	Percent variance	Signif
No. 2	0 days	0.72	51	>0.99	-0.31	9.4	>0.99
No. 5	0 days	0.71	50	>0.99	-0.39	15.0	>0.99
No. 6	0 days	0.65	43	>0.99	-0.35	12.0	>0.99
No. 2	2 days	0.58	33	>0.99	-0.22	5.0	<0.95
No. 5	11 days	0.63	40	>0.99	-0.70	49.0	>0.99
No. 6	11 days	0.80	65	>0.99	-0.70	49.0	>0.99
No. 5	23 days	0.76	58	>0.99	-0.64	41.0	>0.99
No. 6	23 days	0.56	32	>0.99	-0.74	55.0	>0.99
No. 5	44 days	0.56	32	>0.99	-0.56	32.0	>0.99

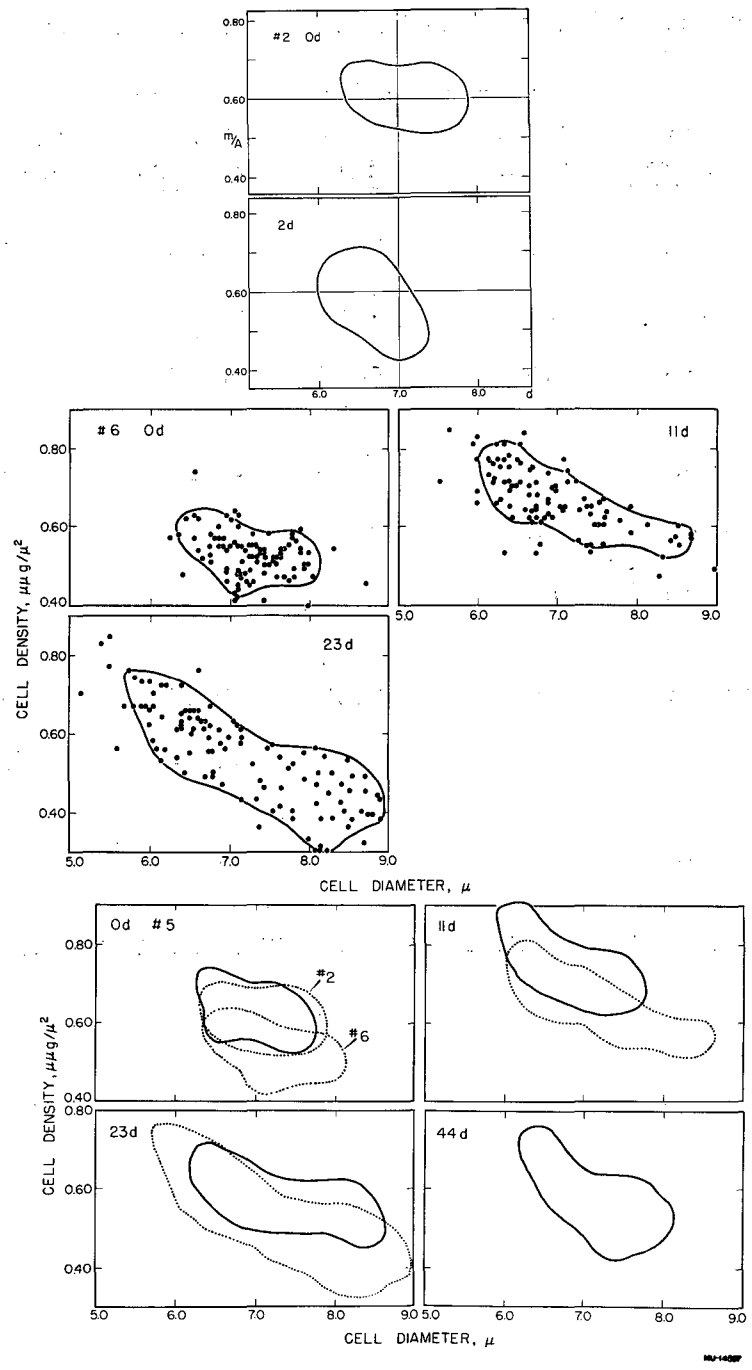

Fig. 21. Scatter diagrams of cellular Hb density vs red cell diameters in control and X-irradiated rabbits.

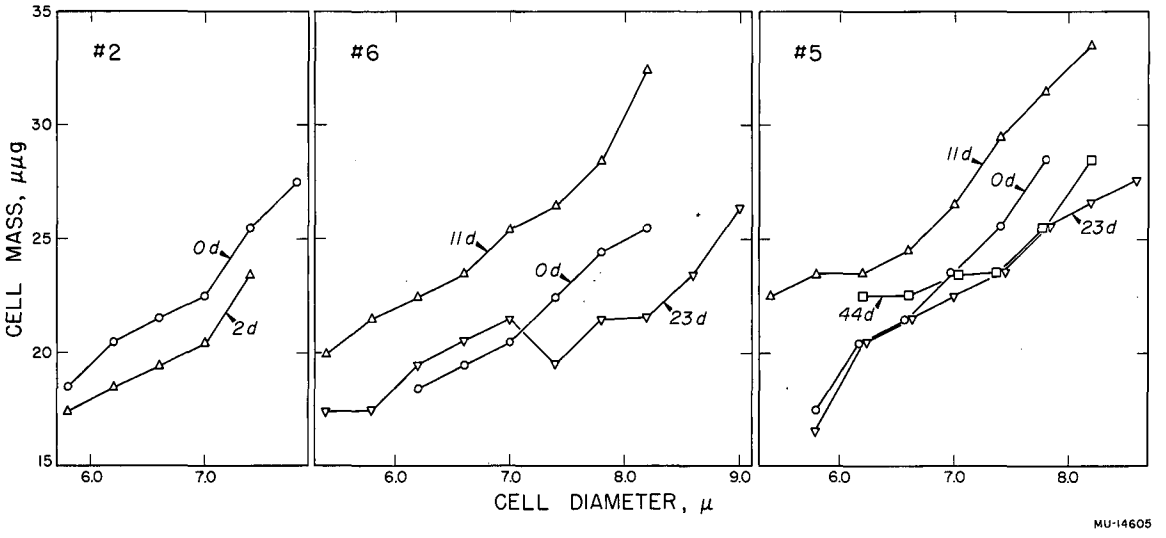

Fig. 22. Median value of Hb content vs red cell diameter in control and X-irradiated rabbits.

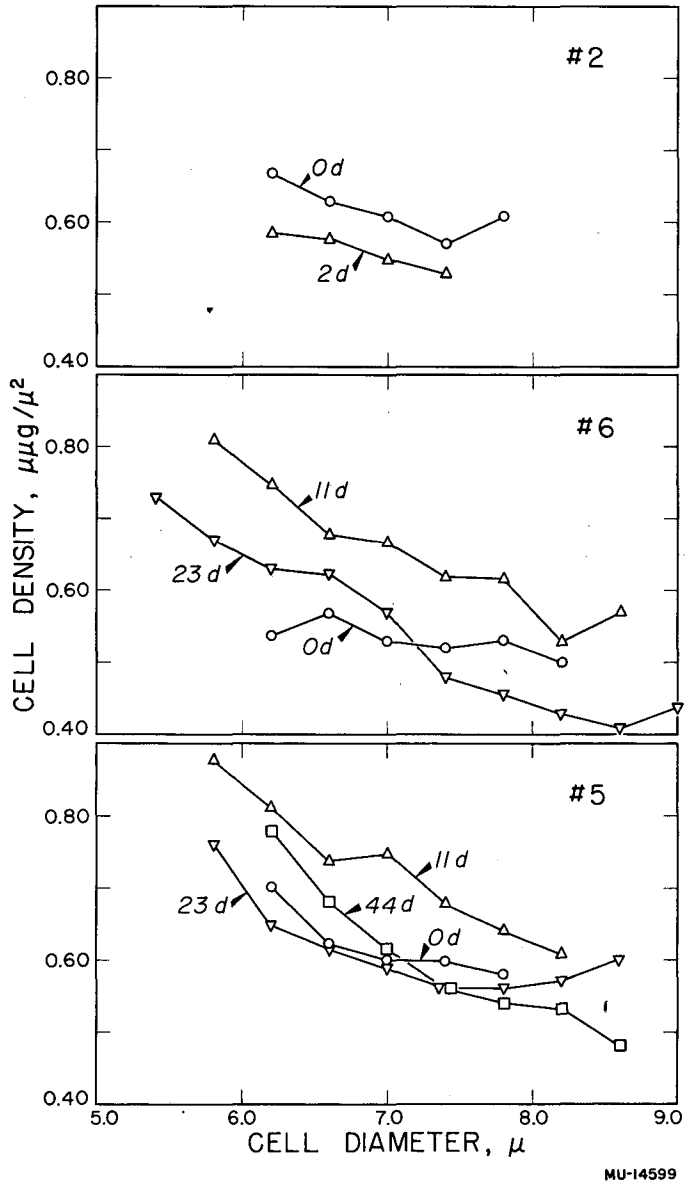

Fig. 23. Median value of Hb density vs red cell diameter in control and X-irradiated rabbits.

usually contain the largest amounts of total hemoglobin, at least in the control populations. That is, in normal populations, macrocytosis overcomes hypochromia in the largest cells, producing cells which are richer in total Hb content than the average of the population as a whole. On the other hand, the smaller cells, though slightly more dense, do not contain as much hemoglobin as the average-sized and larger cells.

It can be seen from the scatter plots of Figs. 20 and 21, and from Figs. 22 and 23, that the normal (0-day) range of Hb density in mass per unit area and the normal total Hb content in cells of the same diameter class was very similar in the 3 animals. For example, cells of 7.0μ diameter contained on the average about 21-23 μμg and showed an average Hb density of 0.54 to 0.60 $\mu\mu g/\mu^2$, and the size range, mass range, and concentration range were about the same in the 3 animals, although the plots for No. 6 show a slight tendency toward a population of larger and less dense cells.

The two-day postirradiation values show a small drop in both the average content and the average density of all the cells. At 11 days postirradiation, both these quantities showed an increase of about 20%, and this was true on the average for all the cells of a given size in a population. The range and degree of scatter between content and density vs cell diameter was also increased at 11 days and still further increased at 23 days. At the latter time, however, the average mass of each size cell had fallen, and was below the normal value for that size in the largest cells, although it was the same or greater in the smallest cells. This appeared to be particularly marked in No. 6, where the density of many of the largest cells was quite low and the average for the population was lower by about 30% than in the pre-irradiation population for that animal. This is shown in the scatter diagram as a larger-than-normal number of cells of high diameter but low mass per unit area and low total mass relative to the mean values. In these plots the quadrants have been drawn through the mean value of both quantities.

If, as before, frequency-distribution curves are plotted for diameters and total Hb content, Fig. 24 is obtained for the diameter distributions of the 3 animals at the different times, and Fig. 25 for the mass distributions. It is seen that a shift in the relative position of the peak in the diameter distribution follows irradiation in all 3 cases. This shift appears to be uniformly downward at 2 days while at 11 days it is further downward and a large part of the population now consists of small cells. At this time a tail of larger cells has appeared which appears to skew the size distribution. At 23 days the effect is further enhanced, so much so in No. 6 that a subpopulation of very large cells forms a separate and distinct class, so widely spaced are the size groups.

The mass-distribution curves show less marked changes but the pattern is opposite. Whereas at 2 days the mass has dropped in the whole population, at 11 days it exceeds the normal values. An increased skewness at the high end also appears, suggesting a larger number of high-content cells relative to the population as a whole. In No. 5 a bimodality is suggested, so great is the proportion of these high-content cells; this is less apparent in No. 6 even though there is a larger group of high-diameter cells in that animal (as discussed above).

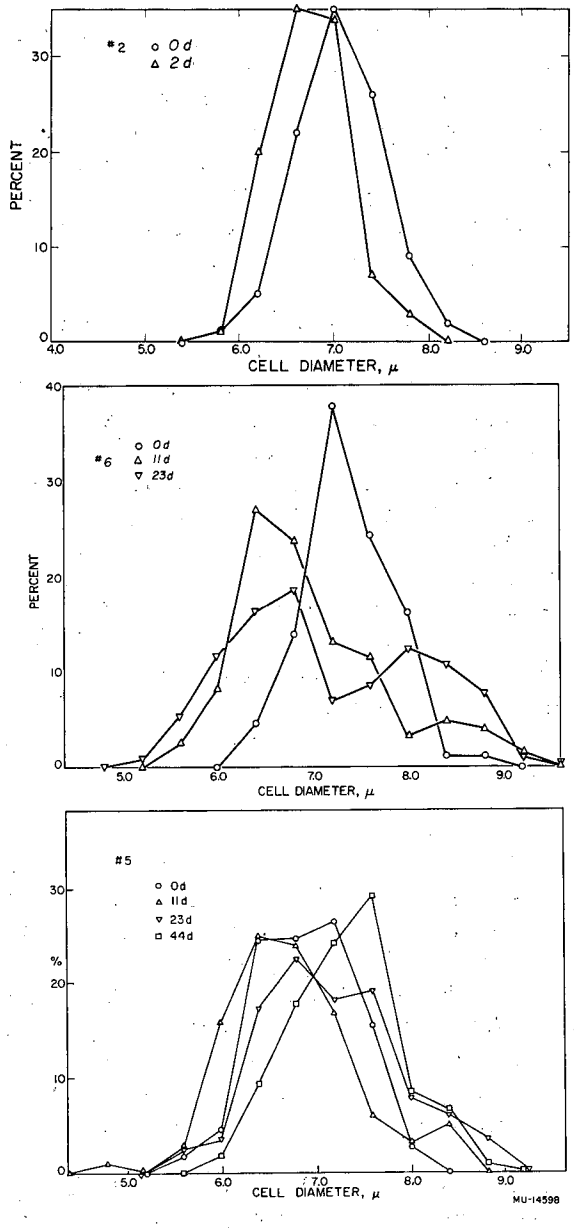

Fig. 24. Frequency distributions of red cell diameters in control and irradiated rabbits.

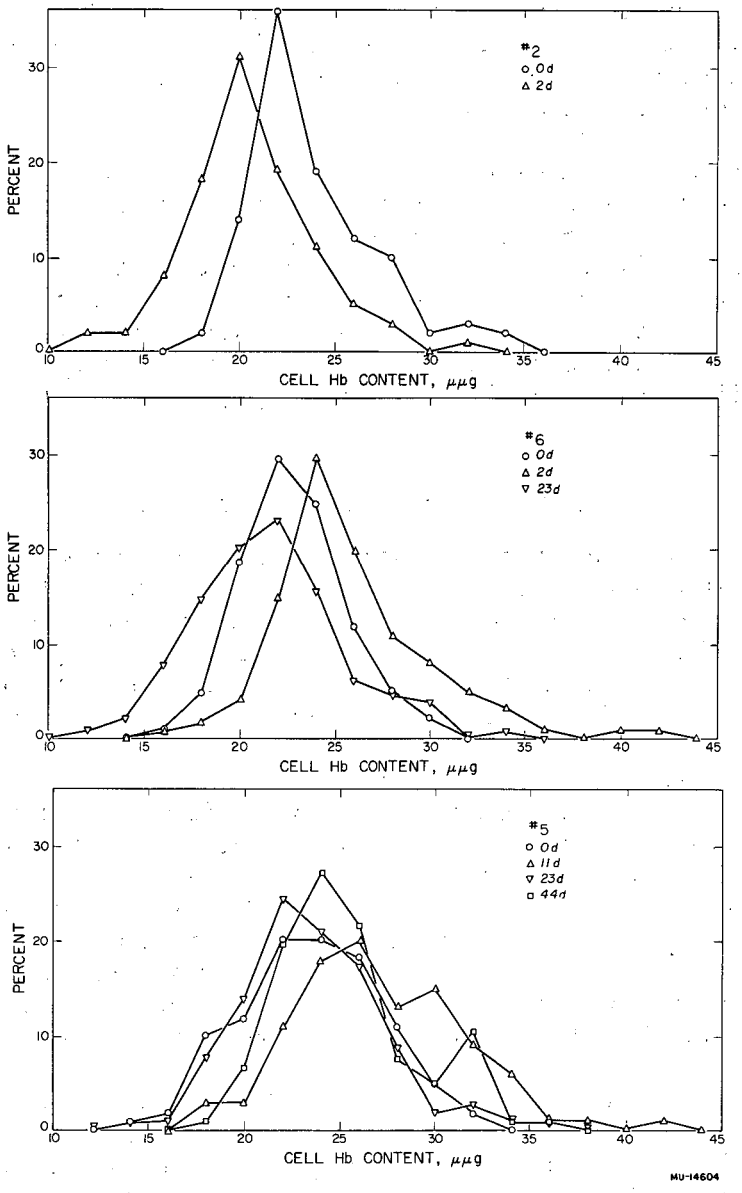

Fig. 25. Frequency distributions of red cell Hb mass in control and irradiated rabbits.

From transforming the frequency distributions into probit diagrams as before, Figs. 26 and 27 result. Differences in the relative positions of the cumulative curves show the changes in the relative proportion of cells in the given size intervals and the changes noted in the previous paragraphs are brought out clearly. The linear "backbone" portions of the curves suggest common distribution parameters; the slopes of these linear portions, generally representing over half of the total population, seem to be substantially the same. Thus the decrease in cell size after irradiation appears to be uniform, and all percentiles of the populations are decreased by the same amount except where the skewness considered as a sub-population is superimposed above the 50% level. The bimodality finally appearing in the 23 day size distribution of No. 6 is well brought out in this way.

In the cumulative mass curves, the initial loss and the uniform increase at 11 days are also apparent. The curves of No. 5 and No. 6 at 0 days do not exhibit the skewness first noted in the normal human populations, but instead, it appears to have developed at 11 days after the irradiation, when regeneration is proceeding. At 23 days the mass distributions are close to the control values once more, there having been a uniform decrease of mass at all percentiles. This decrease between 11 and 23 days appears to be greater in No. 6 than in No. 5; in No. 6 it is about 4 μμg compared to 2 μμg in No. 5.

3. Measurements on Reticulocytes

In an attempt to interpret the changes seen in the population parameters after irradiation, an experiment was carried out in which the youngest mature erythrocytes in the circulating blood, the reticulocytes, were compared with the older cells of the same population with respect to the quantities of Hb content, Hb mass per unit area, and cell diameter. The result of this experiment also bears on the discussion of the human cell populations.

It is known that the average diameters of reticulocytes are larger than those of the older cells in any population, their diameters being variously estimated as between 1.06 and 1.29 times the average of the population as a whole, whatever its value is in a given condition (Persons, 1929). Their average volume has also been found to be greater than that for the population average, while their average Hb concentration is thought to be lower. In an experiment with Fe^{59}-labelled erythrocytes, Borum, Figueroa, and Perry (1957) centrifuged normal blood so labelled from 8 human subjects; the blood was contained in plastic tubes which were frozen after centrifugation and then cut into 4 layers which were counted separately. They found that the activity was highest in the top layer and lowest in the bottom at 15 days after intake of the labelled precursor, while it decreased in the top layer and increased in the bottom during the period 15 to 90 days, and decreased in the bottom thereafter. The ratio Fe^{59} (top)/Fe^{59} (bottom) was greater than 1 in the first 30 days, less than 1 from 60 to 120 days, then again greater than 1. They concluded that the increase in Fe^{59} activity in the bottom layer during this interval indicated a progressive increase in relative density of the cells with age, and its decrease after 90 days indicated the disappearance of senescent cells. The mid-point of the disappearance interval provided an estimate of the mean life span, which was found to be 103-135 days in their material.

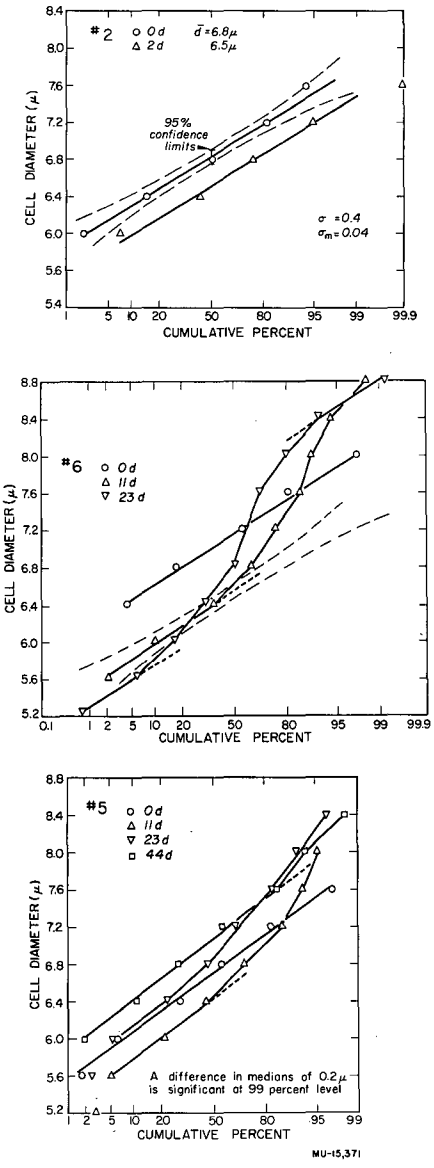

(a)

(b)

(c)

Fig. 26a. Probit diagrams of red cell diameter in control and irradiated rabbits: Rabbit No. 2.

26b. Probit diagrams of red cell diameter in control and irradiated rabbits: Rabbit No. 6.

26c. Probit diagrams of red cell diameter in control and irradiated rabbits: Rabbit No. 5.

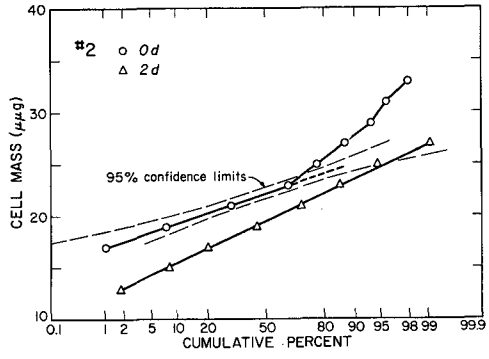

(a)

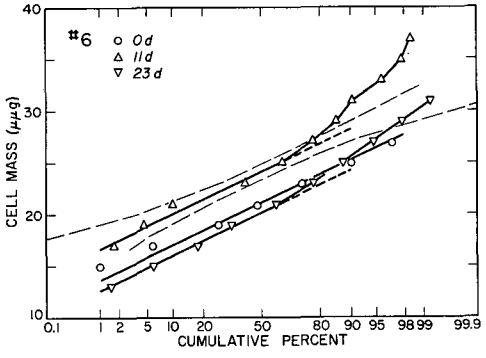

(b)

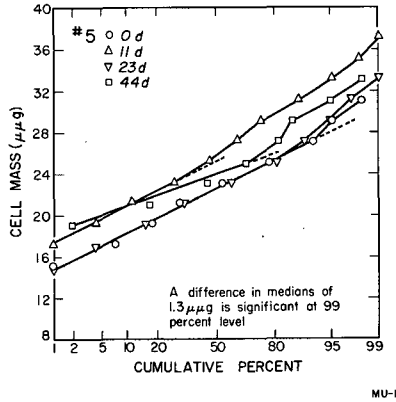

(c)

MU-15,368

Fig. 27a. Probit diagrams of red cell Hb mass in control and irradiated rabbits: Rabbit No. 2.

27b. Probit diagrams of red cell Hb mass in control and irradiated rabbits: Rabbit No. 6.

27c. Probit diagrams of red cell Hb mass in control and irradiated rabbits: Rabbit No. 5.

It also appears well established that the reticulocytes of peripheral blood are still capable of synthesizing some hemoglobin (as discussed in Part I) even though the nucleus has been lost while the cell was still in the late erythroblast stage. The reticulocyte thus seems to be characterized as a large cell in which the concentration of Hb is low and the synthesis is not quite complete, at least in some of the cells. One cannot conclude from the above studies, however, that the resulting total Hb content of reticulocytes is lower than in the older cells, since their larger size may more than counterbalance their lower Hb concentration.

Accordingly, a series of micro-absorption measurements were carried out on the cells contained in the top and bottom layers of centrifuged rabbit's blood. The experiment was performed as follows: 10cc of blood was drawn from the ear of a control rabbit (No. 7), and placed in a centrifuged tube to which had been added 0.1cc of heparin sodium solution (1.0 mg). After gentle agitation, the sample was centrifuged at 3000 rpm for 30 min at 20°C. At the end of this time, the supernatant was clear and straw-colored, indicating that little or no hemolysis had occurred. Using a micropipette, a small sample of cells was withdrawn from the topmost 1 mm of the column of packed cells just underneath the buffy coat. This sample was mixed with a little of the plasma on the surface of a clean microscope slide, a small drop of brilliant cresyl blue dye was added to the mixture, and a thin smear was made in this manner on each of several slides. Using a second micropipette, the procedure was repeated at the lowest 1 mm of the bottom layer, care being taken not to disturb the layering of the column above it. The pipette was wiped clean outside and only the central portion of the sample was used in both cases.

Reticulocyte counts were made on the samples from the top and bottom layers, and the counts showed a relative proportion of 12% in the top layer and less than 1% in the bottom layer. It could thus be concluded that the top layer did contain a large proportion of reticulocytes and other young cells. A series of 8 photographic plates was then exposed, 4 each on the top and the bottom samples. On the top samples, areas were selected in which a number of reticulocytes were visible. Since the smears were thin, it was possible to diagram the positions of the relatively widely spaced cells, and the reticulocyte images were then marked on the photographic plates after development. In this way a total of 50 reticulocytes and other top-layer cells were measured, and 50 cell images randomly selected from the bottom-layer plates were measured for comparison. As before, diameters were measured on the traces, average extinctions were determined, and average densities and total masses were calculated for each cell. The presence of the dye was not felt to have affected the Hb measurement, since it does not appreciably absorb at 415 mμ, and concentrates significantly only in the reticular net of the reticulocytes.

The resulting scatter diagrams of mass vs diameter and density vs diameter are shown in Fig. 28. It can be seen that a distinct separation exists with respect to both quantities, the reticulocytes tending to be highest in both mass and diameter, and lowest in mass per unit area. The other cells from the top layer were intermediate in these values, and the bottom cells showed the reverse properties. The correlation coefficient of mass vs diameter was found to be 0.76, and that for density vs diameter, -0.63, both of which are

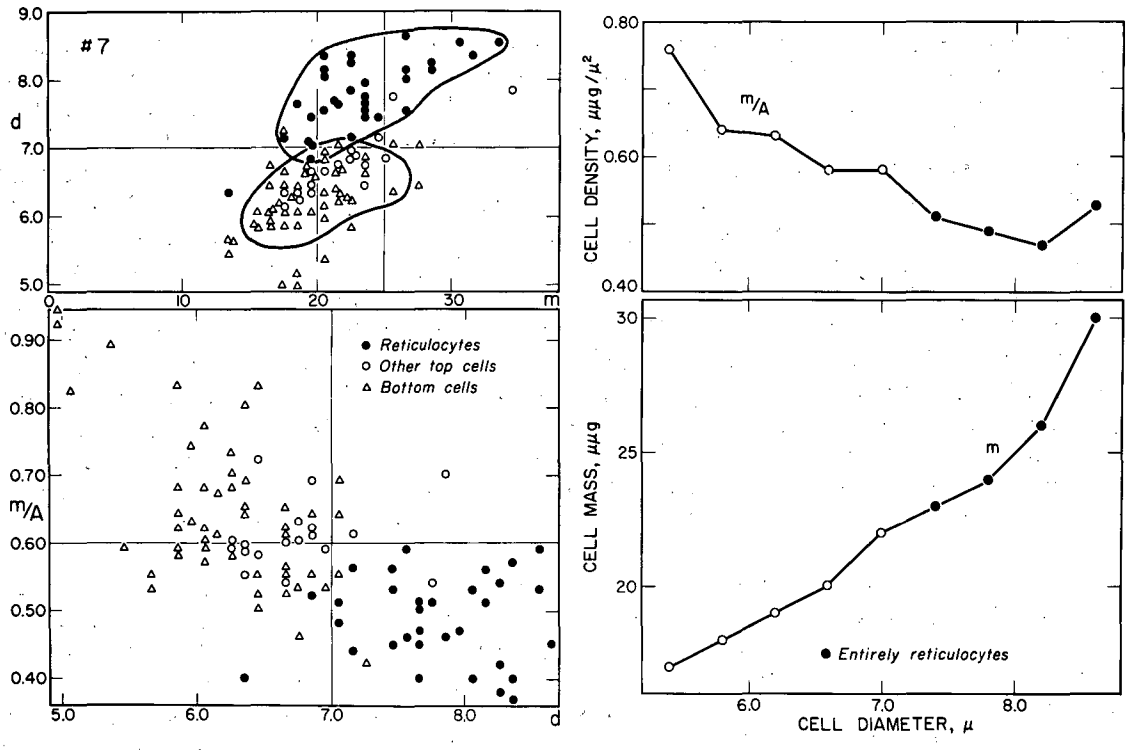

Fig. 28a. Scatter diagrams of cellular Hb mass and Hb density vs cell diameter in young and old red cells of a normal rabbit.

28b. Median values of cell Hb mass and Hb density in young and old red cells of a normal rabbit.

somewhat higher than the values found in the blood samples from the other animals, but this population was, of course, a selected one. However, the average value of cellular hemoglobin content was found to be in good agreement with that found by macrodetermination on the whole blood of this same animal and also on the other 0-day populations, it being 20 μμg, and the average diameter was found to be 6.6 μ, also in close agreement with the other animals. Curves showing the trend in the median values in these quantities are also seen in Fig. 28.

Frequency distributions of cell Hb content and cell diameter are shown in Fig. 29, and are plotted as probit diagrams in Fig. 30. It is seen that the top and bottom cell groups differ significantly in both quantities (a median difference of 0.30 μ and 1.8 μμg was significant at the 99% level for a sample size of 50), and the groups differed most strongly in diameters. The range of values in the two quantities was somewhat greater in the cells from the top layer than in those from the bottom, which is indicated by the greater slopes of the probit curves for the topmost group. The diameters of each subpopulation were normally distributed, while their combination plot indicated bimodality at the 99% level of significance; this also served as a check on the reliability of so interpreting a departure from linearity of this magnitude in the probit curves of all the other cell populations. Evidence of skewness was present at the 95% level of significance in the mass probit curves of both groups and in the curve for the population as a whole.

4. Discussion and Conclusions

As was true of the human cell populations discussed in Part III a, strong qualifications apply to the interpretation of these results with regard to their degree of significance. The number of experiments and the size of the samples were not large enough to eliminate the influence of random variation in any result. However, some inferences may be drawn from the data with some degree of confidence.

1. The results of the reticulocyte measurements are strongly indicative of a greater Hb content in these normal young red cells than exists in the older forms, even though the densities of the young cells are somewhat lower. It may be inferred, firstly, that in general the largest-diameter and lowest-density cells represent the younger cells in any erythrocyte population; it is apparent in Fig. 28 that very little overlap in these parameters occurs in the scatter diagrams. Secondly, there is thus evidence that the red cell not only approaches the spherocyte form with age, i.e., decreases in diameter and increases in density as it grows older, but that there is also either a physical or a functional loss of Hb from the cell as it ages, causing its hemoglobin content to decrease by some 15 or 20% during its lifetime. A rough estimate of the normal rate of loss is obtained by dividing the difference in mass (or diameter for rate of shrinkage) between reticulocytes and the bottom population by the mean life span (Marvin and Lucy, 1917); thus, (21 - 18)/30= 0.1 μμg per day, (7.2 - 6.0)/30 = 0.04 μ/day in the rabbit. This of course assumes a uniform rate, which is probably not the case. However, a difference is already evident between reticulocytes and other young top cells, implying

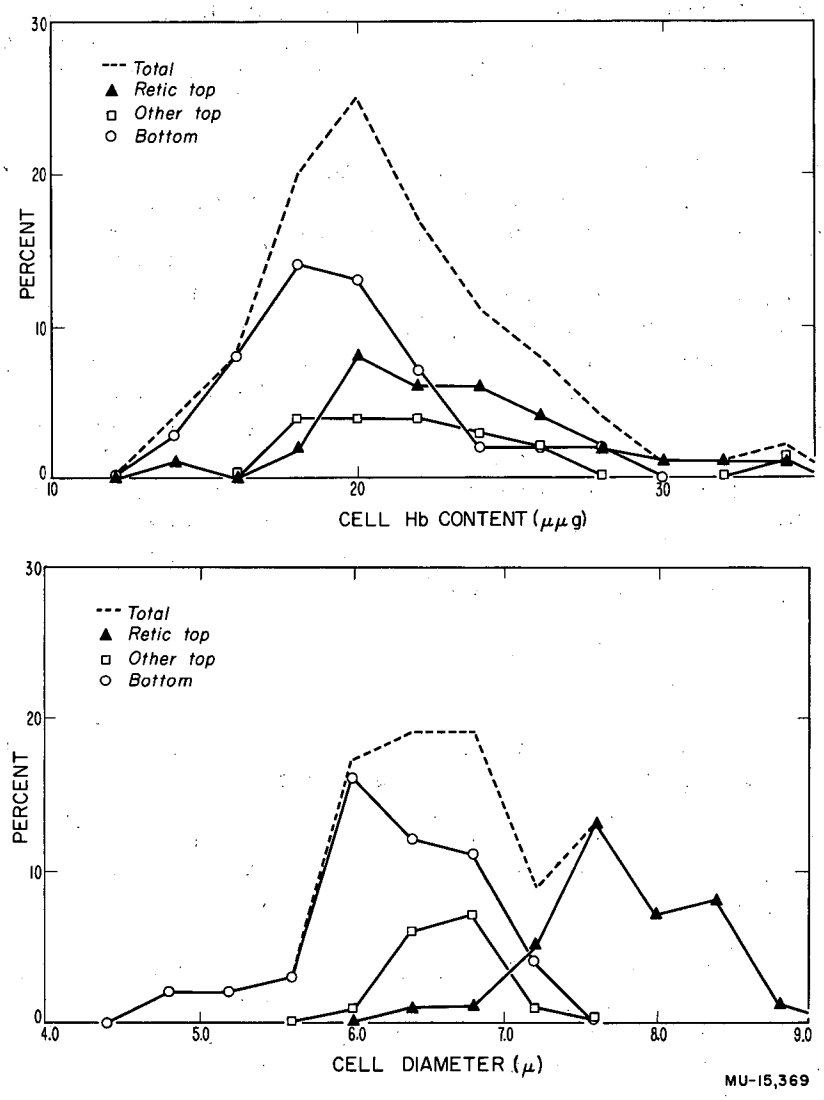

Fig. 29a. Frequency distributions of Hb mass in young and old red cell populations.

29b. Frequency distributions of cell diameter in young and old red cell populations.

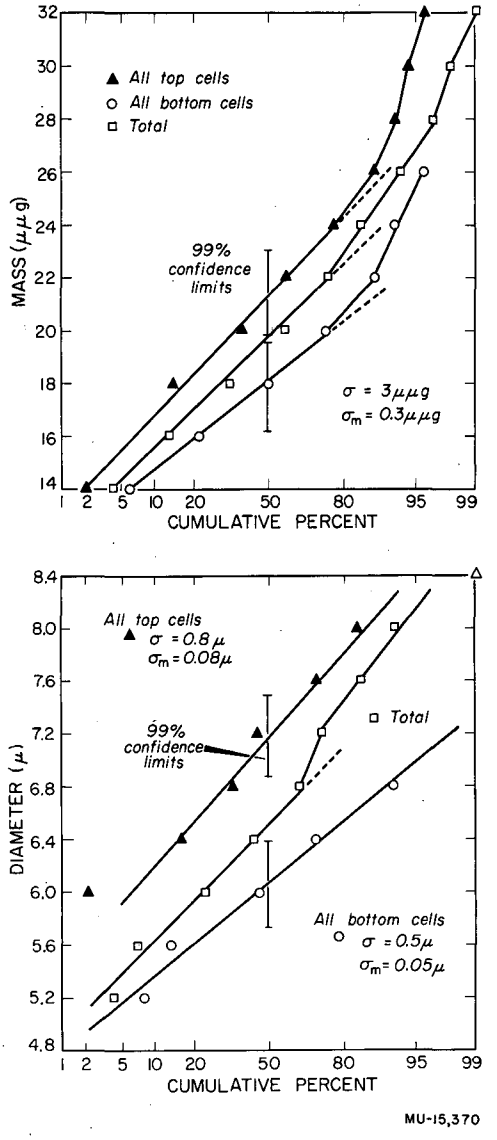

(a)

(b)

Fig. 30a. Probit diagram of cellular Hb mass in young and old red cell populations.

30b. Probit diagram of cell diameter in young and old red cell populations.

that the loss has begun considerably before spherocytosis occurs. Thirdly, the spread in mass values in the largest-size fraction of the cells, those of 8 μ diameter and above, with a range of 20 to 34 μμg total Hb content, may indicate that some of these cells, at least, may have synthesized additional Hb after leaving the marrow before the process of Hb loss became dominant.

2. In any red cell population, a continuous aging of the cell thus results in both size and Hb mass reduction. The 2-day data of the irradiated rabbit No. 2 showed a slight average Hb mass decrease in cells of the same diameter; it suggests that soon after irradiation the aging process has proceeded even faster and without replenishment by any new cells, resulting in a slightly lower median value of both quantities (a mass decrease of 2 μμg, and a diameter decrease of 0.3 μ). There may even have been an increased loss of Hb in some cells per unit diameter reduction. The relatively larger proportion of smaller cells was probably due simply to the fact that the sample was drawn from a smaller parent population in which the same process had occurred, and not that there had necessarily been any absolute increase in the lifetime or numbers of small cells. These changes are significant at the 99% level on the basis of random error alone. They do not appear to correspond to the spherocytosis observed in the guinea pig 7 days after 500 r by Lartigue and Duplan (1956), but they rather resemble the beginning of such a process, which became more evident at later times in the other animals. The spherocytes seen in the centrifuged blood were much smaller, in any case.

3. With the reticulocyte rise following the anemia around 11 days after irradiation, regeneration of the marrow is under way, and many new cells are contributed to the population; Fig. 22 shows that on the average all the cells in the same size ranges are higher in content by 3 to 5 μμg, and have a density which is higher by 0.08 to 0.12 $\mu\mu g/\mu^2$, and Fig. 25 shows further that some of the cells have as much as twice the average Hb content of normal adult red cells. However, the average size of the cells in the population is still lower than in the control populations, at least in the lowest half of the total 11-day population. Hence the total average Hb content per cell in the population has not increased as much as would be expected, though it is seen to be higher by about 3 μμg in these populations. This slight rise was also seen in the other two irradiated animals, for which only average counts were done at 11 days.

4. The new cells (diameter 7.5 to 8.2 μ) are even higher in Hb concentration and Hb content than are their counterparts of the same size range in a control population, which show only about 80% of the density and Hb content shown by these new cells at 11 days. This relative increase may account for the skewness in the mass probit curves for both No. 5 and No. 6 at 11 days. These large cells are still less dense than the population average, but either their thickness or their concentration is greater than that of the young cells of the control populations, and also of the normal reticulocytes measured from rabbit No. 7. In this regard a possible later effect is suggested resembling that observed within 2 days postirradiation by Nizet et al. (1954) and by Bonnichsen and Hevesy (1955), who observed enhanced uptake of Fe^{59} and C^{14} by red cells in vitro shortly after in vivo irradiation. Macrocytosis alone

has often been noted (Jacobsen, 1955) in radiation-induced and other anemias.*

However, the marrow may or may not be able to maintain the rate of Hb synthesis which yields these concentrations in such large cells, even though the large size class continues to be produced; also, of these cells some appear to "age" faster than normally. Thus, at 23 days Fig. 26c shows in No. 5 that the average size has regained its normal level in the lower half of the population and there is now a tail of new, larger cells as well; the concentrations and masses of cells of all sizes are again normal and the mass-distribution curve in Fig. 27c is normal throughout. The bimodality in No. 6, shown in Fig. 26b, suggests that a portion of this 23-day population, the smallest 10 or 15%, might have been the last part of the group of cells which were originally present at 0 days but have been uniformly decreasing in size thereafter, some approaching the spherocyte form at 11 days, while a similar group of large cells was appearing at 23 days. These large cells were between 8 and 9μ in diameter in both No. 5 and No. 6, and in No. 6 there were about 10 times as many at 8μ as in the control population, so that there were enough to constitute a second distinct group, and in No. 6 they did not contribute their share to the total average Hb content of the whole population, and the mass-distribution curve had continued to fall, the median

*Since this study was made, a paper by Ambs has appeared (Acta Haematol. 18, 336, Nov. 1957) in which the reticulocyte crisis was studied in rats with bleeding and phenyl-hydrazine-induced anemias. Microspectrographic measurements showed that many of the young erythrocytes had increased cell diameters and some contained up to 2-1/2 times the average amount of Hb in normal adult red cells. This result tends to confirm the conclusion that the young red cells produced by a regenerating marrow are abnormally high in Hb content, and it indicates that this effect is not peculiar to radiation injury. The measurements on normal reticulocytes reported here suggest that Hb content in the normal young cells rarely exceeds 1-1/2 times the value in the normal adult cells of the same population.

In order to clarify the question of Hb content as a function of cell age, further experiments are planned in which normal red cell populations containing a proportion of labelled cells can be followed both radioautographically and spectrophotometrically during the life span of the cells. With such information a model of the kinetics should then be derivable.

having dropped an average of 4.0 μμg from 11 to 23 days. This is due to the lower content in these large cells relative to their normal counterparts; at 8.5 μ diameter their density is about 0.40 instead of 0.50 $\mu\mu g/\mu^2$ as seen in normal reticulocytes; their masses are about 23 μμg instead of 28 to 30 μμg in the control animal. Some of these large pale cells were target cells, showing the characteristic peak of Hb density in the center; all of these were low in their Hb content.

5. At the same time, the smallest cells, which may be assumed to represent the oldest cells of the population, seem to be in about the normal condition, since the low size ends of all 3 populations show cells with about the same concentration and total content as their normal equivalents. Thus, Fig. 22 shows that the size class of 6.0-μ-diameter cells has a density of 0.60 $\mu\mu g/\mu^2$ and a total content of 18 μμg in No. 6 and No. 2, and a density of 0.70 $\mu\mu g/\mu^2$ and total Hb content of 19 μμg in No. 5. They appear to be normal cells; the slopes of the curves in Fig. 22 are all about the same, with the same degree of correlation of density with diameter. But the relative numbers of these small cells differ; at 11 days 40% of the population was of diameter 6.4μ and below in No. 5 and No. 6, which was the same proportion as at 2 days in No. 2, even with active regeneration proceeding in No. 5 and No. 6. At 23 days this size class had fallen to 20% in No. 5 but had remained at 40% in No. 6. The result in this animal was that one-third of the population still consisted of cells of total content 18 μμg and below, which was only true of 10% of the population in No. 5, which had almost regained the control level. At the same time, more of the cells in No. 5 were of high mass than in No. 6.

6. By this interpretation, the rate of size loss in No. 5 had not been as marked as in No. 6 and the contribution of the group of new cells was sufficient not only to bring the average sizes back to the control level by 23 days, but to exceed it by 44 days. The largest cells no longer have as high an average content and concentration as in the 11-day population, but these quantities are comparable at 44 days to the control values for young cells, and a tail of them is present which skews the population. An "overshoot" effect is thus suggested in the surviving animal. The older, smaller cells also appear to retain slightly more Hb at 44 days. This is suggested by the higher densities at the low-diameter end of the plots in Fig. 22. The correlation of diameter with density is greater for the irradiated animals at the time of marrow regeneration than in their control values; this may also reflect a tendency of the smallest cells to retain more Hb. In No. 2 at 2 days the correlation of diameter with density was lower than normal, which might reflect a lower retention of Hb with age in the early post-irradiation period.

It should be noted that for all these populations, the sample size is about 100, and the standard deviations were all about the same. In the normal control distributions the values found were σ_m = 3.0 μμg and σ_m = 0.4 μ. Under these conditions, the 95% confidence limits of random variation about the theoretical straight line are as plotted on the graph for rabbits No. 2 and No. 6 in Figs. 27 and 28. Thus, at the sample median level, one would expect to find that the values contained in the interval 40 to 60% would include the

true median value for the parent population 95% of the time, while at the 10- and 90-percentile levels, this would be true for the values contained in the interval 4 to 16% and 84 to 96%. Most of the cases where skewness occurred in the curves exceeded these limits at about the 85th percentile, thus indicating that the skewing was significant at the 5% level at that percentile. Such curves occurred in both rabbit and human data.

The same values of population size and standard deviation allow one to estimate the amounts by which both median values and the values of any proportion of two populations must differ in order to be significant at the 95% or 99% level. For the mass-distribution curves this difference was found to be 1.0 μμg at the 95% level and 1.3 μμg at the 99% level when allowance was made for the correlation of masses and diameters in the samples. For the diameter distribution it was found to be 0.18 μ and 0.22 μ at the same levels of significance. The differences in mean Hb content between the three control populations were thus not significant at the 99% level, while the mean diameter difference of No. 6 at 0 days just exceeded this level. The post-irradiation changes in average content and average diameter of the total populations were all significant at the 99% level, and the changes in the high and low regions of the distributions (10 and 90%) were significant at the 95% level.

None of the effects can thus be regarded as real with more than this degree of confidence; in order to materially increase it, however, the experiments would need to be repeated using numbers of cells greater by about a factor of 10 than in these experiments. In order to make measurements on such large numbers of cells, considerably more automation of the method would be required to gather enough data in a reasonable length of time. Experiments combining the method with microradioautography would aid in overcoming this difficulty, and it is planned to attempt them in a future study.

ACKNOWLEDGMENTS

I wish to acknowledge my sincere indebtedness to Professor Cornelius A. Tobias, whose interest, kindness, and continuing support have materially aided all aspects of this work. I am grateful as well to Professors Daniel Mazia and Max Alfert for many stimulating discussions and for their generous and valuable advice. Thanks are also due to the personnel of Donner Laboratory who have offered so many helpful suggestions on frequent occasions; to Mrs. June Barr for her help in some of the determinations, and especially to Mr. Dean Kenyon, who assisted in computation and plate scanning during a part of the work.

I owe particular gratitude to Professor Bo Thorell, for without his guidance, encouragement, and inspiration the study most certainly could not have been undertaken.

Finally, the help and understanding of my wife Carol has been vital at every point, and I have valued it deeply.

* * *

Appreciation is also expressed to the Director of Donner Laboratory and to the Atomic Energy Commission for making equipment and facilities available during the course of the study.

This work was supported in part by the U. S. Atomic Energy Commission.

BIBLIOGRAPHY

1. Adair, G.S., Ogston, A.G., and J.P. Johnston; Biochem. J. 40, 867 (1946).
2. Alfert, M.; J. Cellular Comp. Physiol. 36, 381 (1950).
3. Ambs, E.; Acta Haematol. 15, 302 (1956).
4. Austoni, M.E.; Proc. Soc. Exptl. Biol. Med. 85, 48 (1954).
5. Barer, R.; Nature 169, 366 (1952).
6. Berlin, N.I., Lawrence, J.H. and H.C. Lee; Science 114, 385 (1951).
7. Bloom, M.A. and W. Bloom; J. Lab. Clin. Med. 32, 654 (1947).
8. Blout, E.R., Bird, G.R., and D.S. Grey; J. Opt. Soc. Amer. 40, 304 (1950).
9. Bond, V.P., Cronkite, E.P., Sondhaus, C.A., Imirie, G., Robertson, J.S. and D.C. Borg; Rad. Res. 6, 554 (1957).
10. Bonnichsen, R. and G. Hevesy; Acta Chemica Scand. 9, 509 (1955).
11. Borum, E.R., Figueroa, W.G. and S.M. Perry, Clin. Res. Proc. 5, 1 (1957).
12. Bussi, L., Pozza, G. and A. Bernasconi; Biol. Latina 7, 576 (1954).
13. Caspersson, T.; Skand. Arch. Physiol. 73, Suppl. 8 (1936).
14. Caspersson, T.; Cell Growth and Cell Function, Norton, N.Y. (1950).
15. Davies, H.G.; Discussions Faraday Soc. 9, 442 (1950).
16. Davies, H.G. and M.H.F. Wilkins; Nature 169, 541 (1952).
17. Davies, H.G., and P.M.B. Walker; Progress in Biophysics 3, 195 (1953).
18. Davies, H.G., Wilkins, M.H.F., and R.H.G.B. Boddy; Exp. Cell Res. 6, 550 (1954).
19. Dervichian, D.G. and C. Magnant; Ann. Inst. Pasteur 73, 841 (1947).
20. Doan, C.A., Cunningham, R.S., and F.R. Sabin; Contributions to Embryology 16, 163 (1925). (Carnegie Inst. Publications).
21. Doniach, I., Howard, A., and S.R. Pelc; Progress in Biophys. 3, 1 (1953).

22. Dyson, J.; Nature 164, 229 (1949).

23. Engström, A.; Progress in Biophysics, 1, 164 (1950).

24. Engström, A. and B. Lindstrom; Biochimica et Biophysics Acta 4, 351 (1950).

25. Gilmour, J.R.; J. Path. Bact. 52, 25 (1941).

26. Glick, D., Engström, A. and B.G. Malmstrom; Science 114, 253 (1951).

27. Hennessy, T.G and R.L. Huff; Proc. Soc. Exptl. Biol. Med. 73, 436 (1950).

28. Huff, R.L. Elmlinger, P.J., Garcia, J.F., Oda, J., Cockrell, M.S., and I.H. Lawrence; J. Clin. Invest. 30, 1512 (1951).

29. Hyden, H. and H. Hartelius; Acta Psychiat. et Neurol. Suppl. 48 (1948).

30. Jacobsen, L.O., Hagen, C.W. and R.E. Zirkle; USAEC Ayrb MDDC-1174 (1947).

31. Jacobsen, L.O., Marks, E.K., and E. Lorenz; Radiology 52, 371 (1949).

32. Jacobsen, L.O., in Radiation Biology, Ed. Hollaender, N.Y., McGraw-Hill, 1954.

33. Jope, E.M.; Hemoglobin, Butterworths, London (1949).

34. Kahn, J.B. and J. Furth; USAEC Rept. ORNL-1186 (1952).

35. Kohler, A.; Z. Wiss. Mikroskop. 21, 129, 275 (1904).

36. Lagerlöf, B., Thorell, B. and L. Åkerman; Exp. Cell Research 10, 752 (1956).

37. Lartigue, O., and J.F. Duplan; Rev. Franc. Etudes Clin. et Biol. 1, 861 (1956).

38. Lemberg, R. and J.W. Legge; Hematin Compounds and Bile Pigments, Interscience, N.Y., (1949).

39. London, I.M., Shemin, D., West, R., and D. Rittenberg; J. Biol. Chem. 179, 463 (1949).

40. Marvin, H.N. and D.D. Lucy; Acta Hemotol. 18, 239 (1957).

41. Maximow, A.A.; In Special Cytology (Coudry) 2nd ed., Vol. II.

42. Mazia, D., Plaut, W.S. and G. Ellis; Exp. Cell Res. 9, 305 (1955).

43. Moberger, B.; Acta Radiol. Scand. Suppl. 114 (1954).

44. Nizet, A., Lambert, S., Herve, A., and F.M. Bacq; Arch. Intern. Physiol. 52, 129 (1954).

45. Nizet, A. and S. Lambert; Bull. Soc. Chim. Biol. 35, 771 (1953).

46. Odeblad, E.; Acta Radiol. Suppl. 93 (1952).

47. Oster, G. and A.W. Pollister; Physical Technique in Biological Research, Academic Press, N.Y. (1956).

48. Patau, K.; Chromosoma 5, 341 (1952).

49. Persons, E.L.; J. Clin. Invest. 7, 615 (1929).

50. Perutz, M.F.; Nature 161, 204 (1948).

51. Pollister, A.W. and H. Ris; Cold Spring Habor Symp. Quant. Biol. 12, 147 (1947).

52. Ponder, E. and W.G. Millar; Quart. J. Exp. Physiol. 14, 67 (1924).

53. Ponder, E. and G. Saslow; Quart. J. Exp. Physiol. 19, 319 (1929).

54. Ponder, E., Hemolysis and Related Phenomena, Girme and Stratton, N.Y. (1948).

55. Price-Jones, C.; Red Cell Diameters, Oxford Medical Publications, London (1933).

56. Prosser, C.L., Painter, E.E., Lisco, H., Brues, A.M., Jacobsen, L.O. and M.N. Swift; Radiology 49, 269 (1947).

57. Ross, M.H., Furth, J. and R.R. Bigelow; Blood 7, 414 (1952).

58. Shemin, D. and D. Rittenberg; J. Biol. Chem. 166, 627 (1946).

59. Shillaber, L.P.; Photomicrography, Wiley, N.Y. (1944).

60. Swift, H.; Proc. Natl. Acad. Sci. (U.S.) 36, 643 (1950).

61. Swift, H. and E. Rasch; Physical Technique in Biological Research, Academic Press, N.Y. (1956).

62. Thorell, B.; Acta Med. Scand. Suppl. 200 (1947).

63. Thorell, B.; Disc. Faraday Soc. 9, 432 (1950).

64. Walker, P.M.B.; Physical Technique in Biological Research, Academic Press, N.Y. (1956).

65. Wasserman, L. R., Lawrence, J. H., Berlin, N. I., Dobson, R. L. and S. Estren; Acta Med. Scand. 143, 442 (1952).

66. Wintrobe, M. M.; Clinical Hematology, Lea and Febiger, Philadelphia, 1952.